# ROLE OF TWO *POPULUS TRICHOCARPA* ENDO-β-1,4-GLUCANASES AND THEIR ARABIDOPSIS ORTHOLOGS IN PLANT CELL WALL DEVELOPMENT

by

Magdalena Hrynkiewicz-Moczulski

BSc, The University of British Columbia, 2009

A THESIS SUBMITTED IN PARTIAL FULFILLMENT OF

THE REQUIREMENTS FOR THE DEGREE OF

MASTER OF SCIENCE

in

THE FACULTY OF GRADUATE STUDIES

(Forestry)

THE UNIVERSITY OF BRITISH COLUMBIA

(Vancouver)

September 2012

# Abstract

Plant cell walls are imperative to the normal growth and development of plants as they serve many functions, including protecting the protoplast and providing rigidity to the stem. In this study two poplar and Arabidopsis endoglucanases, which have been hypothesized to play a role in secondary cell wall development, were examined. The Class B endoglucanases, PtGH9B5 and AtGH9B5, are secreted enzymes that have a predicted GPI anchor, while the Class C endoglucanases, PtGH9C2 and AtGH9C2, are also predicted to be secreted but contain a carbohydrate-binding module (CBM). The poplar endoglucanases were up-regulated in Arabidopsis using a 35S promoter as well as the Arabidopsis CesA8 promoter, respectively. Additionally, Arabidopsis t-DNA insertion lines of each Arabidopsis gene were analyzed, and an RNAi construct was created to down-regulate AtGH9C2 in Arabidopsis. All of the transgenic plant lines were examined for changes in cell morphology and patterning, growth and development, cell wall crystallinity, microfibril angle, and proportion of cell wall carbohydrates. Mis-regulation of PtGH9B5/AtGH9B5 resulted in changes in glucose and xylose content, suggesting that this endoglucanase may be involved in regulating the amount of cellulose and/or xylans in the developing secondary cell wall. Furthermore, mis-regulation of PtGH9C2/AtGH9C2 resulted in a change in crystallinity, which was inversely correlated with a change in plant height and rosette diameter. This suggests that this endoglucanase may be involved in modifying cell wall crystallinity at the time of primary growth cessation and/or early secondary cell wall development. Together, these results support the role of these endoglucanases in secondary cell wall development, though their exact enzymatic function remains to be discovered.

# Table of contents

# List of tables

## List of figures

## Acknowledgements

I would like to thank my very supportive family and friends for sticking with me through this often challenging time. I've learned a lot throughout the last three years and I owe much of that to my fantastic lab members. There was always someone who was willing to guide me in the right direction or explain a new concept and for that I am truly grateful. There are too many names to list, so please accept my sincere thank you and my best wishes for your future endeavours.

# Chapter 1: Introduction

## 1.1 Overview

As the plant stem grows and develops new cells are added successively from the vascular cambium. Xylem, the water-conducting tissue of the stem, is produced to the inside of the cambial zone, while phloem, the main photosynthate-transporting tissue, is produced outwards. Cell division relies on the careful construction of a new cell wall between two cells. The plant cell wall has many functions, including: defining cell shape, protecting the protoplast, cell adhesion, maintaining normal water balance and turgor pressure, as well as regulating the diffusion of macromolecules (Trainotti et al., 1999). Industrially, the cell wall has many uses, including being the starting material for pulp and paper manufacture, lumber, synthetic fibres, and biofuels, all of which are dependent on the synthesis of the intricate lignocellulosic network of the secondary cell wall. Over the last few decades, a significant amount of research has been devoted to elucidating the role(s) of various proteins in synthesizing plant cell walls. Among the many enzymes studied to date, plant β-1,4-D-endoglucanases (glycosyl hydrolase family 9, EC 3.2.1.4) have recently been receiving much attention. By definition, these endoglucanases are capable of cleaving the β-1,4-D-glucan bonds adjoining glucose moieties characteristic of cell wall polysaccharides, such as cellulose and xyloglucan.

## 1.2 Cellulose

The plant cell wall is made up of an intricate network of cellulose, hemicellulose, pectin, various proteins, and lignin (more specifically in secondary walls). The cellulose microfibrils are the main load-bearing structures of the cell wall, and are composed of linear chains of β-1,4-D-glucose, with the primary repeating unit being cellobiose. Individual glucan chains are unbranched, and as such permit extensive intra- and inter-molecular hydrogen bonding among

associated chains in close proximity to one another. This latter feature ultimately results in the formation of both crystalline and amorphous regions within the cellulose microfibrils. These same glucan chains also have the capacity to interact with other plant cell wall polysaccharides and lignin via free hydroxyl groups, forming what is commonly defined as lignin-carbohydrate-complexes (LCC).

Cellulose microfibrils are believed to be synthesized by the cellulose synthase complexes at the plasma membrane (Cosgrove, 2005). In *Arabidopsis thaliana*, there are ten cellulose synthase (CesA) genes encoding the proteins that make up the cellulose synthase complex. The cellulose synthase complex has been shown to have a hexameric rosette structure, with each rosette predicted to consist of 6 CesA proteins (Cosgrove, 2005). Each cellulose synthase complex is predicted to extrude as many as 36 individual glucan chains, which putatively associate to form a cellulose microfibril 3-5 nm in width. Different CesA proteins make up the cellulose synthase complexes inherent to the primary and secondary walls. Bimolecular fluorescence complementation and immunoprecipitation studies have determined that CesA1, CesA3, and CesA6 likely make up the cellulose synthase complex in primary cell walls (Desprez et al., 2007), and evidence suggests that CesA6 is functionally redundant with CesA2, 5 and 9 (Desprez et al., 2007; Persson et al., 2007). It has been suggested that these redundant CesAs may function in different developmental stages or tissue types. The secondary cell wall cellulose synthase complexes consist of CesA4, CesA7, and CesA8 (Taylor et al., 2003), and mutations in any one of these CesA proteins results in an irregular xylem (*irx*) phenotype, where the xylem appears to be collapsed as a result of a deficiency in cellulose (Taylor et al., 2004; Turner & Somerville, 1997). Additionally, microarray studies investigating the expression of CesA4, CesA7, and CesA8

reveal that they are highly expressed in plant stems and weakly expressed in leaves, seedlings, flowers, and roots (Hamann et al., 2004), further implicating these proteins in secondary cell wall development.

## 1.3 Cell wall polysaccharides

Unlike cellulose, hemicelluloses are heteropolymeric residues and have several different side chains preventing them from forming crystalline macromolecules (Caffall & Mohnen, 2009). They can also be acetylated and contain sugar acids, such as glucuronic and galacturonic acids. Hemicelluloses are synthesized in the Golgi apparatus and transported by vesicles to the cell wall where they are thought to interact with cellulose to create a cellulose-hemicellulose network. Although the details of this interaction are still unclear, hemicelluloses are thought to either directly or indirectly tether cellulose microfibrils, strengthening the cell wall (Cosgrove, 2005). Cross-linking of cellulose by the hemicellulose xyloglucan has been well-studied, and it is generally though that this interaction is important in providing mechanical strength in primary cell walls but also the necessary extensibility to allow for cell expansion (Whitney et al., 1999).

Pectin forms a hydrated gel matrix in which the cellulose-hemicellulose network is embedded during primary cell wall biosynthesis. Pectins are complex polysaccharides rich in galacturonic acid that are often augmented by various side chains (Caffall & Mohnen, 2009). Homogalacturonan (HG) and rhamnogalacturonan II (RGII) have a galacturonic acid backbone, however, HG is not substituted, while RGII may have a combination of four distinct side chains. RGI has a backbone of repeating rhamnose and galacturonic acid residues, and may also have various side chains. Pectins, like hemicelluloses, are synthesized in the Golgi apparatus and transported to the plasma membrane via vesicles, where they are released into the cell wall.

## 1.4 Primary and secondary cell walls

The primary cell wall is generally composed of approximately 20-30% cellulose, 30-35% pectin, and 25-30% hemicelluloses (Albersheim et al., 2011) with the principal hemicellulose in dicotyledonous primary cell walls being xyloglucan (Caffall & Mohnen, 2009). The role of the primary cell wall is to maintain the shape of the cell while remaining flexible enough for the cell to undergo expansion, which may account for why primary cell walls tend to have less cellulose and more pectin and hemicelluloses than secondary cell walls. Once expansion has ceased, the secondary cell wall begins to be deposited, strengthening the cell and solidifying its final shape.

In contrast to the primary cell wall, the secondary cell wall of angiosperms is generally composed of 37-57% cellulose, 17-30% lignin, 20-37% hemicellulose, and less than 10% pectin (Albersheim et al., 2011). The most abundant hemicelluloses are glucuronoxylans and glucomannans (Caffall & Mohnen, 2009). Additionally, once the secondary cell wall is deposited, it is often lignified, which precedes programmed cell death. Lignin is a complex macromolecule composed of phenylpropanoid moieties that are extremely recalcitrant and form a relatively impermeable layer around the cell wall polysaccharides, further strengthening the cell wall (Pilate et al., 2004). Together, the strength, extensibility, and thickness of plant cell walls depends on the proportion and organization of the cell wall components.

In the case of parenchymous tissue, a lack of a secondary cell wall enables the cells to assume the shape required of them by neighbouring cells, as well as become a source for new cells that may be required after wounding (Albersheim et al., 2011). In cells that do develop a secondary cell wall, the timing of the wall's development largely depends on the pattern of cell expansion occurring in a particular cell. Cells that exhibit tip growth, such as root hairs and pollen tubes,

may start depositing a secondary cell wall at one end of the cell while the other end is still rapidly expanding (Taiz & Zeiger, 2006). Some plant cells exhibit diffuse growth where cell expansion is evenly distributed; however, certain cell types such as fibres, exhibit an intermediate form of expansion between tip and diffuse growth.

## 1.5 Cellulose crystallinity

Cellulose crystallinity is an important aspect of plant cell walls as it determines both the physical strength of the wall, as well as its recalcitrance to enzymatic breakdown (Mansfield et al., 1999). As mentioned previously, cellulose exists in crystalline and amorphous forms, and the amorphous regions enable its cross-linking to associated cell wall carbohydrates such as xyloglucan, but these regions also expose it to enzymatic attack via cellulases secreted by organisms such as fungi (Libertini et al., 2004). However, amorphous regions are necessary for flexibility of the plant stem to abiotic factors such as wind, as well as cell expansion during periods of growth (Fujita et al., 2011; Harris & DeBolt, 2008). Crystalline cellulose, in conjunction with the lignification of secondary cell walls, helps to provide the plant with the tensile strength needed to remain upright as well as stand up to the turgor pressure in xylem (Maloney et al., 2012). Cell wall crystallinity can vary greatly among plant species and developmental stages. For example, grasses have been measured as having 51-58.5% crystallinity, which is higher than the leaves of most other species and is more similar to the crystallinity observed in Arabidopsis stems (Harris & DeBolt, 2008). This variation in cell wall crystallinity can affect the tensile strength of cellulose, as well as the rate of cell expansion, as higher cell wall crystallinity has been shown to have a limiting effect on the total expansion of cells in hypocotyls (Fujita et al., 2011; Harris & DeBolt, 2008).

## 1.6 Microfibril angle

Another cell wall attribute important in determining the flexibility of plant stems is the microfibril angle of cellulose in xylem secondary cell walls. In gymnosperm fibres and angiosperm vessels and tracheids, secondary cell walls are deposited in three distinct layers known as S1, S2, and S3 (Preston, 1974). The S1 and S3 layers are thinner and tend to have a larger MFA while the S2 layer is significantly thicker and tends to have a smaller MFA (Barnett & Bonham, 2004). Due to the thickness of the S2, MFA measurements made on a wood and/or a plant stem sample tend to result in an approximation of the MFA of this layer, which makes up approximately 94% of the entire secondary cell wall. The smaller the angle of the cellulose microfibrils in relation to the long axis of the cell, the stiffer the stem. Therefore, it follows that juvenile wood of saplings tends to have a large MFA which helps young trees survive wind stress and snow load conditions early on in their lifespan, while mature wood tends to have a smaller MFA to support the girth of the full grown stem and crown (Barnett & Bonham, 2004).

## 1.7 Cell expansion

Cell expansion relies on the controlled separation of cellulose microfibrils, followed by cell water uptake and addition of new cell wall polysaccharides (Somerville, 2006). There are several proteins hypothesized to play central role(s) in this process. Expansins are a group of proteins that have been found to induce cell expansion when applied exogenously to plants, as well as when applied to isolated cell walls (Cosgrove, 2005). Although the exact mechanism by which expansins achieve this is not known as they do not have a known catalytic function. However, it is thought that they are able to interrupt the hydrogen bonds adhering adjoining cellulose and hemicellulose, thereby allowing the cellulose microfibrils to slide apart (Cosgrove, 2005). Xyloglucan endotransglycosylase/hydrolase (XTH) enzymes are capable of both cleaving

and ligating xyloglucan chains (XET activity), as well as chain shortening (XEH activity), operating with dual functionality (Eklof & Brumer, 2010; Rose et al., 2002; Teeri & Brumer, 2003; Vissenberg et al., 2005). Through this action, XETs have been suggested to be involved in not only wall loosening but wall strengthening, as well as incorporation of newly synthesized xyloglucan into the cell wall (Eklof & Brumer, 2010). Degradation of pectin during cell expansion by enzymes such as pectate lyases and polygalacturonases may enable the incorporation of newly synthesized cell wall components (Marin-Rodriguez et al., 2002). During early growth cessation, pectin methylesterases (PMEs) have been proposed to increase the ability of pectin to form calcium cross-links, resulting in a stiffer cell wall (Caffall & Mohnen, 2009). Furthermore, pectin may also form a pectin-protein network with the (hydroxy)proline-rich glycoprotein extensin. This structural protein has been found to be down-regulated during cell expansion and up-regulated during growth cessation, as the cell wall stiffens (Cannon et al., 2008). Finally, a group of enzymes called endo-1,4-β-D-glucanases are also hypothesized to play a role in cell expansion. Although their function in cell wall synthesis/remodelling is largely unknown, they are capable of cleaving β-1,4-glycosidic bonds such as those found in cellulose and xyloglucan (Lopez-Casado et al., 2008).

## 1.8 Plant 1,4-β-D-endoglucanases

Endo-1,4-β-D-glucanases exist in many different organisms including bacteria, fungi, termites, and plants (Libertini et al., 2004). Microbes that degrade the cellulose polymer into its monomeric subunits as a carbon source produce endoglucanases that generally contain a cellulose binding domain (CBD) that aids in the degradation of crystalline cellulose. In contrast, most plant endoglucanases lack a CBD, and are therefore hypothesized to act on the

amorphous regions of cellulose or non-crystalline polysaccharides such as xyloglucan (Wilson & Urbanowicz, 2010). Plant endoglucanases belong to glycosyl hydrolase family 9 (GH9) (Cantarel et al., 2009), which contains enzymes capable of breaking β-1,4 glycosidic bonds within a glycan chain (Wilson & Urbanowicz, 2010). In *Arabidopsis thaliana*, there are currently 25 genes coding for endoglucanases, and according to Urbanowicz et al. (2007) these endoglucanases can be divided into three structural subclasses: A, B, and C. Given the various chemical properties of the plant endoglucanases, they have been hypothesized to a play a variety of roles in cell wall biosynthesis and modification, including cell elongation and differentiation, cytokinesis, organ abscission, and fruit ripening (Libertini et al., 2004).

### 1.8.1 Class A endoglucanases

Class A endoglucanases are membrane-bound and include a long N-terminal extension, linked to a catalytic domain. In Arabidopsis, there are three genes that code for membrane-bound endoglucanases, termed *KORRIGAN (KOR), KOR2, and KOR3* (Molhoj et al., 2001; Nicol et al., 1998). There is evidence of *KOR* playing a role in both primary (Lane et al., 2001) and secondary cell wall development (Szyjanowicz et al., 2004). For example, in the *irx2* mutants of *KOR*, it was found that the secondary cell wall was defective; in particular, cellulose synthesis in the xylem was decreased, as was the cellulose crystallinity (Szyjanowicz et al., 2004). Although the phenotypic effects of *KOR* are unmistakable, the specific role it plays in cell wall biosynthesis is still under debate. It has been suggested that *KOR* is involved in removing a sitosterol-β-glucoside precursor molecule from the elongating cellulose chain (Peng et al., 2002), however, several studies have reported results to the contrary (as discussed in Maloney & Mansfield, 2010). While *KOR* expression can be seen throughout the entire plant, *KOR2* and *KOR3* tend to

be expressed in specific tissues. *KOR2* expression has been noted in the proximal parts of leaves and flower organs, trichomes, and root hairs within the root differentiation zone, while *KOR3* expression has been measured in trichome support cells as well as bundle sheath cells surrounding the vascular bundles within leaf mesophyll tissue (Molhoj et al., 2001).

### 1.8.2 Class B endoglucanases

Class B endoglucanases are predicted to be secreted enzymes, and consist of a signal peptide, followed by a catalytic domain. These enzymes make up the bulk of the Arabidopsis GH9 family with 19 members, and have been linked to a variety of different developmental roles. One such Arabidopsis endoglucanase, *CEL1* (At1g70710), was found to be highly expressed in young developing tissues, particularly in thickening cell walls of xylem (Shani et al., 2006). Additionally, Tsabary et al. (2003) showed that *cel1* anti-sense plants had mechanically weaker stems and a significant decrease in cellulose and lignin content. Research examining *Eucalyptus globulus* secondary growth has provided evidence of the up-regulation of *EG1* (Arabidopsis ortholog At2g32990) and *EG3* (Arabidopsis ortholog At4g39010) in the phloem of juvenile wood (Goulao et al., 2011). Furthermore, several microarray studies have alluded to potential roles for Class B endoglucanases, including the up-regulation of At1g22880, At2g44570, and At2g32990 in response to IAA application (Goda et al., 2004), or the high level of expression of At4g39000 in stamen, pistil, seeds, and ovules (Xie et al., 2011).

### 1.8.3 Class C endoglucanases

Finally, Class C endoglucanases are structurally similar to Class B endoglucanases, but also contain a carbohydrate binding module (CBM) at their C-terminus. This CBM is unique to plants and has been classified as CBM49 (Urbanowicz et al., 2007). Many CBMs are hypothesized to

facilitate the binding of these enzymes to crystalline cellulose, but it has yet to be shown what role, if any, the plant CBM49 plays in cell wall synthesis (Shoseyov et al., 2006). The three members of Class C have not been well-studied in Arabidopsis, however, the tomato and rice orthologs of At1g64390 (AtGH9C2) have been examined. For example, Urbanowicz et al. (2007) provided evidence for the binding of the tomato SlCel9C1 CBM to crystalline cellulose, as well as hydrolysis of artificial cellulosic polymers, and a variety of plant cell wall polysaccharides by the catalytic domain. A similar study was performed on the orthologous rice endoglucanase, further confirming that the catalytic domain is capable of hydrolyzing various polysaccharides. However, contrary to the tomato study, the authors provided evidence suggesting that the CBM is post-translationally cleaved (Yoshida & Komae, 2006b). Therefore, the role of CBM49 is still uncertain, and the other two members of Class C do not provide any clues as they remain largely unstudied.

## 1.9 Goals and hypotheses

Since endoglucanases have long been predicted to play a role in the modification of cell walls of several different plant organs, the goal of this research project was to identify endoglucanases which may specifically contribute to secondary cell wall development in plant stems. *Arabidopsis thaliana* and *Populus trichocarpa* were chosen as model organisms in this study, as Arabidopsis has a short life cycle, while poplar is an excellent model system for secondary growth and wood formation. By examining recent poplar transcriptome data for endoglucanases highly expressed during active xylem development in 20 poplar clones, two candidate genes were chosen for investigation. In order to identify the poplar endoglucanases within the transcriptome data set, the Arabidopsis GH9 family was blasted against these

sequence data. Although the poplar ortholog of At5g49720 (KOR) showed the highest overall expression in xylem, the orthologs of At1g19940 (AtGH9B5) and At1g64390 (AtGH9C2) were chosen as they showed the next highest expression and had not been previously well-studied. Additionally, these two genes showed high expression in transcriptome data from *Eucalyptus globulus* xylem, and a similar trend was seen in Arabidopsis expression data (Winter et al., 2007). In order to verify that the correct poplar orthologs were chosen, a phylogenetic tree containing Arabidopsis and predicted poplar glycosyl hydrolase family 9 protein sequences was constructed (Figure 3.1). This analysis confirmed that the poplar gene orthologous to At1g19940 is POPTR_0005s25890, and the poplar gene orthologous to At1g64390 is POPTR_0003s13940. In keeping with the endoglucanase nomenclature proposed by Urbanowicz et al. (2007), I will be referring to POPTR_0005s25890 as PtGH9B5, and POPTR_0003s13940 as PtGH9C2. I chose the last number in the common name based on the current nomenclature of the corresponding Arabidopsis orthologs (AtGH9B5 and AtGH9C2). The following chapters were devoted to the study of both endoglucanases, and are briefly described below.

### 1.9.1 Chapters 2-5: Methodology, results, discussion, and conclusions

The goal of this research was to determine if PtGH9B5 and PtGH9C2 play a role in secondary cell wall development. The hypothesis was that if these genes play a role in secondary cell wall development, alterations in their level of expression would have a phenotypic effect on plant growth form and/or cell wall properties and ultrastructure. This was tested by examining Arabidopsis plants with varied expression of these genes, as well as YFP localization of the native Arabidopsis promoters. Arabidopsis t-DNA insertion mutants in AtGH9B5 and AtGH9C2

were ordered from the Arabidopsis Biological Resource Centre and several overexpression plant lines were developed to drive the expression of PtGH9B5 and PtGH9C2 in wild-type Arabidopsis. One overexpression plant line employed the 35S promoter, while the other used the Arabidopsis CesA8 promoter in order to specifically drive expression in secondary cell walls. Additionally, an RNAi construct was developed to suppress AtGH9C2 expression in Arabidopsis plants. All plants were analyzed for changes in plant growth form, differences in cell structure of plant stem cross-sections, cell wall crystallinity, microfibril angle, and structural carbohydrate content.

# Chapter 2: Methodology

## 2.1 Selection of poplar genes and Arabidopsis orthologs

The poplar genes examined in this study were chosen based on expression levels in a xylem transcriptome study, where 20 unrelated poplar genotypes undergoing active xylem development were subject to RNA sequencing (Geraldes et al., 2011). The Arabidopsis endoglucanase family was blasted against the poplar transcriptome data to identify the poplar endoglucanases. The Arabidopsis ortholog At5g49720 (KOR, AtGH9A1) had the highest expression in xylem with 2220 gene copies per tree. The next most highly expressed endoglucanases were AtGH9B5 (At1g19940) with 502 gene copies per tree and AtGH9C2 (At1g64390) with 134 gene copies per tree. The latter two endoglucanases were therefore chosen for further study, as KOR has already been well researched. In order to determine if the correct poplar and Arabidopsis orthologs had been chosen, a neighbour-joining 1000 bootstrap phylogenetic tree was constructed using the entire Arabidopsis GH9 family as well as the predicted poplar GH9 family. The tree was rooted by using *Selaginella moellendorffii* (XP_002985347) as the outgroup.

## 2.2 Arabidopsis t-DNA mutants

The t-DNA mutant seed lines SALK_121501 and CS25087, with a t-DNA insertion in the promoter of AtGH9B5 and in an exon of AtGH9C2 respectively, were obtained from The Arabidopsis Information Resource (TAIR, www.arabidopsis.org). Mutant seeds were first sterilized for 2 minutes in 70% ethanol, followed by 8 minutes in 10% sodium hypochlorite, and then washed four times with sterile water. After four days at 4°C, seeds were plated on half MS medium (Murashige & Skoog, 1962) with no sugar and 50mg/L kanamycin sulphate (Invitrogen Canada Inc., Burlington, ON). After 10 days, seedlings were planted in autoclaved soil and

placed in a growth chamber under a 16/8-h light/dark cycle at 21°C. Each plant was screened for homozygosity of the t-DNA insertion by extraction of genomic DNA from leaf tissue via a quick genomic DNA extraction protocol (described below) and subsequent PCR. Primers were designed using the t-DNA primer design website hosted by the SALK Institute Genomic Analysis Lab (SIGNAL; http://signal.salk.edu/tdnaprimers.2.html). Seeds were collected from only those plants that were identified as homozygous.

## 2.3 Overexpression construct development

The *P. trichocarpa* genes PtGH9B5 and PtGH9C2 were isolated from *P. trichocarpa* cambium cDNA using the primers listed in Table 2.1. Primers were designed to work with the pENTR/D-TOPO vector (Invitrogen Canada Inc., Burlington, ON), and therefore the nucleotides "CACC" were added to the forward primers and three random base pairs were added to the beginning of the reverse primers. The 35S overexpression vector pH7YWG2 (Karimi et al., 2005) consists of a 35S promoter, a GATEWAY cloning site, and a C-terminal YFP. LR Clonase Enzyme II (Invitrogen Canada Inc., Burlington, ON) was used to ensure GATEWAY directional cloning of each poplar gene and correct insertion of each gene was confirmed by genomic DNA PCR sequencing of the plasmids.

A second over-expression construct was designed to specifically regulate the expression of the poplar genes in the secondary cell walls, by swapping the 35S promoter in the pH7YWG2 vector with the Arabidopsis CesA8 (At4g18780) promoter. The Arabidopsis CesA8 promoter (AtCesA8pr) was cloned from *A. thaliana* Col-0 leaf genomic DNA using primers originally designed by Dr. Lisa McDonnell (Ph.D. thesis in the Mansfield laboratory), but modified to include a SacI restriction site on the forward primer and a SpeI restriction site on the reverse

primer (Table 2.1). These restriction enzymes were used to excise the AtCesA8pr fragment from pENTR, as well as cleave the pH7YWG2 vector. Both fragments were run on an agarose gel then isolated by the Invitrogen Gel Extraction Kit (Invitrogen Canada Inc., Burlington, ON). T4 DNA Ligase (Fermentas Canada Inc., Burlington, ON) was used to ligate the AtCesA8 promoter into the pH7YWG2 vector. Correct insertion of the AtCesA8 promoter was confirmed by sequencing. LR Clonase Enzyme II (Invitrogen Canada Inc., Burlington, ON) was used for GATEWAY directional cloning of PtGH9B5 and PtGH9C2 into the modified vector, as previously described. Again, appropriate insertion of the poplar genes was confirmed by DNA sequencing of the plasmids.

Table 2.1. List of cloning, screening, and qPCR primers.

| Primer Name | Sequence (5' to 3') | Use |
|---|---|---|
| PtGH9B5 FW | CACCATGGAGAAGTTTGTGAGGCTC | Cloning/Screening |
| PtGH9B5 RV | CGATCAGGCCAAAGTGTAGCTTG | Cloning/Screening |
| PtGH9C2 FW | CACCATGGTGAAGTTTGCGAGGC | Cloning/Screening |
| PtGH9C2 RV | CGATCAGGTCAGACTGTAGCTTGAAAC | Cloning/Screening |
| AtCesA8pr FW | GTCGAGCTCTCACAATCTTCTTCCTGGTCG | Cloning |
| AtCesA8pr RV | GTTACTAGTTTGGAGAAACAGAGAAATG | Cloning |
| AtGH9B5pr FW | GTCGAGCTCCACAGTAGAGAAGGCACTGGAA | Cloning |
| AtGH9B5pr RV | GTTACTAGTCGAGAATGACGACGATTCAAGAG | Cloning |
| AtGH9C2pr FW | GTCATCGATGCCATTGTCATCTTGGCATGAG | Cloning |
| AtGH9C2pr RV | GTTCCTAGGAAGTGGCCGGAGAAGGAGAG | Cloning |
| YFP FW | GTCGGCGCGCCATGGTGAGCAAGGGCGAGGA | Cloning/Screening |
| YFP RV | GTTGAGCTCCTTGTACAGCTCGTCCATGCCGAGAGT | Cloning/Screening |
| RNAi con FW | GGGGACAAGTTTGTACAAAAAAGCAGGCTTACCGATCCGTCAGCGGTTA | Cloning/Screening |
| RNAi con RV | AAGAGCACTTCCGTAGTTATAGTACTCCGCCACCTGGTGTCTTCTGAATG | Cloning |
| RNAi 48930 FW | CTCGAGGAACATTCAGAAGACACCAGGTGAGCGGAGTACTATAACTACG | Cloning |
| RNAi 48930 RV | GGGGACCACTTTGTACAAGAAAGCTGGGTGTTGAGGATGAGCCTTGATG | Cloning/Screening |
| RT EF1α FW | TCCAGCTAAGGGTGCC | qPCR |
| RT EF1α RV | GGTGGGTACTCGGAGA | qPCR |
| RT PtGH9B5 FW | GCGAAGGATTCGCTCAAG | qPCR |
| RT PtGH9B5 RV | CCTCTTCTCGGTCATGTCT | qPCR |
| RT PtGH9C2 FW | GGTGCTGTCTACTCTGACTA | qPCR |
| RT PtGH9C2 RV | CAACCATGTAACTAGTAGCTCTC | qPCR |
| RT AtGH9C2 FW | GCGGTATCCAGCTACACT | qPCR |
| RT AtGH9C2 RV | TTCTTGACGAACCAGAGGTAA | qPCR |
| RT At1g48930 FW | ACTTACCAGCTTCCTCAATG | qPCR |
| RT At1g48930 RV | GGCCACCTTGTACATAGAC | qPCR |
| RT At4g11050 FW | CAGCTTCTTCTCCTAGTCC | qPCR |
| RT At4g11050 RV | GGACCGTATAGCTTGGTGAT | qPCR |

## 2.4 Promoter-YFP construct development

In order to isolate the AtGH9B5 and AtGH9C2 promoters (AtGH9B5pr and AtGH9C2pr), primers were designed to amplify approximately 1500bp upstream of the AtGH9B5 and AtGH9C2 start codons, respectively (Table 2.1). The sequence "CACC" was added to the forward primers, and three random nucleotides were added to the reverse primers in order for the fragments to be compatible with the pENTR vector. The subsequent cloned fragments were confirmed by sequencing. The promoter-fusion vector pMDC110 (Curtis & Grossniklaus, 2003) was modified by replacing the GFP with the YFP gene, which was isolated from the pH7YWG2 vector. Primers for the YFP were designed with the restriction enzyme AscI on the forward primer and SacI on the reverse primer (Table 2.1). These restriction enzymes were employed to cleave the pMDC110 vector and excise the YFP fragment. Both fragments were run on an agarose gel and isolated via the Invitrogen Gel Extraction Kit (Invitrogen Canada Inc., Burlington, ON). T4 DNA Ligase (Fermentas Canada Inc., Burlington, ON) was used to ligate the YFP into pMDC110 and correct insertion was confirmed by DNA sequencing. LR Clonase Enzyme II (Invitrogen Canada Inc., Burlington, ON) was used for GATEWAY directional cloning of the AtGH9B5 and AtGH9C2 promoters into the modified pMDC110 vector. Correct insertion of the promoters was verified by sequencing.

## 2.5 RNAi down-regulation construct development

The RNAi construct was designed to simultaneously suppress the expression of all three Class C GH9 endoglucanases in Arabidopsis: AtGH9C2, At1g48930, and At4g11050. To do so, two cDNA fragments approximately 300bp long were cloned and PCR overlap was used to join them. One fragment was cloned from AtGH9C2 and was designed to suppress both AtGH9C2 and At4g11050, which represents the most highly conserved region between the two genes as

determined by BioEdit's "Find conserved regions" function disallowing gaps (BioEdit, Ibis Biosciences, Carlsbad, CA, USA). This region was located at 679bp - 879bp on the AtGH9C2 cDNA sequence (Phytozome v7.0, 2011). The second fragment was designed to suppress At1g48930 and was located at 76bp - 406bp on the At1g48930 cDNA sequence (Phytozome v7.0, 2011). Primers for the two fragments were designed to facilitate PCR overlap by adding the first 30bp of the At1g48930 fragment to the reverse primer of the AtGH9C2/At4g11050 fragment, and by adding the last 30bp of the AtGH9C2/At4g11050 fragment to the forward primer of the At1g48930 fragment (Table 2.1). To facilitate GATEWAY directional cloning of the joined fragment into pHELLSGATE, the forward primer of AtGH9C2/At4g11050 fragment had a 5' and 3' attB1 pDONR site added, and the reverse primer of the At1g48930 fragment had a 5' and 3' attB2 pDONR site added (primers in Table 2.1).

The AtGH9C2/At4g11050 and At1g48930 fragments were cloned from *A. thaliana* cambial cDNA and confirmed by sequencing. In order to facilitate PCR overlap of the fragments, a PCR reaction was run using 2µl of each fragment's gel extract as well as the forward primer of the AtGH9C2/At4g11050 fragment and the reverse primer of the At1g48930 fragment. The PCR product was run on an agarose gel and the resulting 600bp band was purified. The joined fragment was cloned into the pDONR vector using BP Clonase II (Invitrogen Canda Inc., Burlington ON). Correct insertion of the fragment into pDONR was confirmed by sequencing. LR Clonase Enzyme II (Invitrogen Canda Inc., Burlington ON) was used to insert the fragment into the destination vector pHELLSGATE, and correct insertion was verified using the restriction enzymes XhoI and XbaI, as well as by DNA sequencing of the plasmids (Helliwell & Waterhouse, 2003).

## 2.6 Agrobacterium transformation

Transformation of the 35S::PtGH9B5, 35S::PtGH9C2, AtCesA8pr::PtGH9B5, AtCesA8pr::PtGH9C2, AtGH9B5pr::YFP, AtGH9C2pr::YFP, and RNAi::AtGH9C2 constructs into the Agrobacterium strain GV3101 was carried out using a freeze-thaw method. In short, approximately 1µg of each plasmid was added to one 50µl aliquot of GV3101 cells and incubated on ice for 30 minutes. The cells were heat-shocked in a 37°C heat block for 5 minutes then 1mL of YEP liquid medium was added to each tube. Tubes were shaken at 220rpm at 28°C for 2 hours then centrifuged at 13000rpm on a bench-top centrifuge for 1 minute. The supernatant was discarded and the cells were resuspended in 100µl liquid YEP medium, then spread on YEP plates containing either 50mg/L rifampicin and spectinomycin for the overexpression constructs and RNAi construct, or 50mg/L rifampicin and kanamycin sulfate for the AtGH9B5PR::YFP construct. Colonies were grown in a 28°C incubator for 2 days at which point potential positive transformants were screened by PCR. Positive colonies were stored as glycerol stocks in a -80°C freezer.

## 2.7 Transient expression of AtGH9B5pr::YFP and AtGH9C2pr::YFP in Arabidopsis

The functionality of the AtGH9B5pr::YFP and AtGH9C2pr::YFP constructs was tested by performing Agrobacterium-mediated transient expression in 4-day old wild-type Arabidopsis seedlings. In brief, cocultivation medium consisting of liquid MS media (Murashige & Skoog, 1962) with 1% sugar was prepared in advance and Agrobacterium cultures were grown overnight at 28°C and 220rpm. An aliquot of each culture was added to 20mL of cocultivation medium in a petri dish to an $OD_{600}$=0.3. Approximately 30 Arabidopsis seedlings were added to each plate, at which point the plates were covered in aluminum foil and allowed to incubate for

two days at room temperature. After two days, seedlings were screened for presence of YFP using fluorescence microscopy.

## 2.8 Plant transformation

*A. thaliana* wild-type Col-0 seeds were sterilized for 2 minutes in 70% ethanol, followed by 8 minutes in 10% sodium hypochlorite, and then washed four times with sterile water. Seeds were placed in a refrigerator at 2°C for four days and then plated on half MSO medium (Murashige and Skoog, 1962) with no carbon source. After growth on plates for ten days, seedlings were planted in autoclaved soil and placed in a growth chamber under a 16/8-h light/dark cycle at 21°C.

Plant transformation was carried out according to a modification of the protocol by Clough and Bent (1998). Basically, 200mL of each Agrobacterium culture was grown overnight at 28°C and 220rpm in liquid YEP media containing 50mg/L rifampicin and spectinomycin for the overexpression constructs and RNAi construct, or 50mg/L rifampicin and kanamycin sulfate for the native promoter YFP constructs. Cultures were harvested by centrifugation and resuspended in a 5% sucrose solution to an $OD_{600}$ of approximately 0.8 and then 12.5µl of Silwet L-77 was added to each 50mL aliquot of culture. Cultures were sprayed directly onto Arabidopsis flowers. Inoculated plants were covered with black garbage bags for 16 to 24 hours. The transformation procedure was repeated every 4-5 days as long as immature flowers remained, generally two or three times in total. Once plants matured, seeds were collected in bulk.

Seeds were screened for potential transformants by plating them on half MSO media without a carbon source containing 25mg/L hygromycin for all constructs except the RNAi construct to which 75mg/L kanamycin sulfate was added to the media. Potential transformants were planted in soil and allowed to self. Each plant was treated as an individual line and had its seeds collected separately. Three to five lines of each construct were chosen for further study.

## 2.9 Transgenic plant growth

Transgenic and wild-type seeds were sterilized and stratified as described previously, then plated on half MSO medium (Murashige & Skoog, 1962) and no carbon source. The media also contained 25mg/L hygromycin as selection for the transgenic seeds. After growing on plates for ten days, seedlings were planted in autoclaved soil and placed in a growth chamber under a 16/8-h light/dark cycle at 21°C.

## 2.10 DNA screening

Transgenic plant lines were screened by PCR to verify the presence of the construct in each plant line. DNA was extracted from leaves via a quick genomic DNA extraction protocol (Edwards et al., 1991). In short, each leaf sample was ground in 350µl of extraction buffer and vortexed for 10 seconds. The samples were centrifuged in a bench-top centrifuge at 13000rpm speed for 3 minutes then 300µl of the supernatant was transferred to a new tube containing 300µl of isopropanol. The solution was mixed by inversion and left at room temperature for 20 minutes, at which time the samples were centrifuged at 13000rpm for 5 minutes. The supernatant was discarded and the pellet was washed with 500µl of 70% ethanol, then the samples were spun at 13000rpm for 1 minute. The supernatant was discarded and the pellet was air-dried for 20 minutes, and then resuspended in sterile water. For the overexpression

constructs, the primers that were used to isolate the PtGH9B5 and PtGH9C2 genes were also used for screening, similarly, the RNAi fragment primers were used to screen the RNAi plants, and the primers used to isolate the YFP from pH7YWG2 were used to screen the native promoter YFP plants (Table 2.1).

## 2.11 Microscopy

Transgenic and wild-type plant stems were cross-sectioned by hand approximately 1cm from the base of 4 week old plants, and stained with 0.5% toluidine blue stain for 2 minutes, then washed twice with distilled water. Sectioning was repeated on a weekly basis until plants reached 8 weeks of age. The cross-sections were mounted in water on a glass slide with cover slip. Slides were viewed using a Leica DMR light microscope (Leica Microsystems Inc., Ontario, Canada) equipped with a QImaging Qicam camera (QImaging, British Columbia, Canada) operated via OpenLab software (PerkinElmer Inc., Massachusetts, USA). For the transient expression analysis, the same microscope was used to excite YFP using a 450-490nm laser with emissions passing through a 515 band filter.

Stable promoter::YFP transformants were mounted in water on a glass slide with coverslip and examined using a Leica DMI6000 (Leica Microsystems Inc., Ontario, Canada) inverted microscope connected to a Hamamatsu 9100-02 EMCCD camera (Hamamatsu Corporation, New Jersey, USA). Improvision Volocity software (PerkinElmer Inc., Massachusetts, USA) was used to capture images. YFP fluorescence was detected on the same microscope equipped with a Perkin Elmer Ultraview VoX Spinning Disk Confocal with FRAP System (PerkinElmer Inc., Massachusetts, USA). YFP was excited with a 514nm laser and emissions passed through a 540/30 band filter.

## 2.12 RNA isolation and cDNA production

Total RNA was extracted from leaf tissue for the overexpression constructs using TRIzol (Invitrogen Inc., Burlington, ON) according to the manufacturers' instructions. To remove DNA, RNA was treated with TURBO DNase (Ambion, Burlington, ON, Canada). In place of inactivation buffer, 5µl 27.5mM EDTA was added to each reaction and heated at 75°C for 5 minutes. The concentration and A260/280 of the DNA-free RNA was determined using a Nanodrop 1000 (Thermo-Fischer Scientific Inc., Wilmington, DE, USA). 1µg of DNA-free RNA was transcribed to cDNA using iScript cDNA Synthesis Kit (Bio-Rad Laboratories Canada Ltd., Mississauga, ON, Canada). The quality of cDNA was tested by performing PCR using EF1α reference gene primers (Table 2.1).

## 2.13 Quantitative PCR

The *Arabidopsis thaliana* reference genes UBQ5, EF1α, and eIF4A (Gutierrez et al., 2008) were tested for their level of expression and optimal annealing temperature using a gradient cycle on a C1000 Thermal Cycler Bio-Rad CFX96 Real-Time PCR System (Bio-Rad Laboratories Canada Ltd., Mississauga, ON, Canada). The reference gene EF1α was chosen as it had the highest level of expression and its optimal annealing temperature most closely aligned with the annealing temperature of the quantitative PCR primers for the PtGH9B5, PtGH9C2, At1g48930, At4g11050 and AtGH9B5 genes (Table 2.1).

The cDNA used in qPCR was diluted by one third and each plant cDNA sample was run in triplicate using the gene-specific primers and the EF1α primers simultaneously. Three plants of each plant line were tested, as well as three wild-type plants. Gene expression was measured on a C1000 Thermal Cycler Bio-Rad CFX96 Real-Time PCR System (Bio-Rad Laboratories Canada

Ltd., Mississauga, ON, Canada) using SsoFast EvaGreen Supermix (Bio-Rad Laboratories Canada Ltd., Mississauga, ON, Canada) according to the manufacturers' instructions. Relative expression of the poplar gene was determined by using the formula: $2^{-(Cq_{sample} - Cq_{reference})}$ (Coleman et al., 2009).

## 2.14 Microfibril angle and crystallinity

The microfibril angle (MFA) of five Arabidopsis stems from each overexpression transgenic line was measured using an X-ray diffraction technique (Ukrainetz et al., 2008). The bottom 3cm of 8-week old plant stems was used for analysis. The 002 diffraction spectra of each stem was screened for T-value distribution and symmetry on a Bruker D8 discover X-ray diffraction unit equipped with an area array detector (GADDS). Wide-angle diffraction was used in the transmission mode, and measurements were made with CuKα1 radiation (λ=1.54 Å). The X-ray source was fit with a 0.5 mm collimator and the scattered photon was collected by a GADDS detector. The X-ray source and the detector were both set at a theta angle of 0°. The diffraction data was integrated using GADDS software and further analyzed to estimate MFA values.

Cell wall crystallinity was determined on the same stems used for measuring MFA, using the same X-ray unit and parameters as for the MFA measurements, except the source theta was set at 17°. The diffraction data were integrated using GADDS software and the output data further analyzed using a crystallinity calculation program based on the Vonk method (Vonk, 1973).

## 2.15 Cell wall chemical analysis

A micro Klason procedure was used to measure the amount of structural carbohydrates in stems of several lines of each overexpression and RNAi construct as well as wild-type Arabidopsis. The bottom 10cm of 8 week old Arabidopsis stems was collected and dried in a

50°C oven for two days. Stems were pooled for each line as well as wild-type, and then ground in a Wiley Mill to pass a 40-mesh (0.4mm screen). Ground tissue was placed in filter paper pockets and extracted overnight with hot acetone using a Soxhlet apparatus. Approximately 10mg of extracted ground stem tissue was treated with 100µL of 72% $H_2SO_4$ for 5 minutes, then vortexed and spun briefly on a bench-top centrifuge. The sample was incubated for 1 hour at 30°C, then 2mL of nanopure water was added and the sample was vortexed again. After incubation at 140°C for 75 minutes, the samples were centrifuged for 4 minutes, then the supernatant was removed for structural carbohydrate analysis. The carbohydrate contents were determined by anion exchange on a high performance liquid chromatography machine (Dx-600; Dionex, Sunnyvale, CA, USA) equipped with an ion exchange PA1 (Dionex) column, a pulsed amperometric detector with a gold electrode, and a SpectraAS3500 auto injector (Spectra-Physics). Glucose, xylose, mannose, galactose, arabinose and rhamnose were eluted with water at 1 mL/min, and detection was achieved by pulsed amperometry with post-column addition of 200 mM NaOH at 0.5 mL/min. Sugar concentrations were calculated from standard curves created from external standards.

## 2.16 Statistical analysis

Differences in measurements of wild-type and transgenic plant height, rosette diameter, crystallinity, and MFA were analysed for statistical significance using the SAS 9.2 software package (SAS Institute Inc., Cary, NC, USA). Each dataset was imported separately and analysed against wild-type using the “PROC GLM” statement. Significant differences among the means were measured using the “MEANS” statement and “LSD” option, which performs pairwise t-tests equivalent to Fisher’s least-significant-difference test. Differences among average

measurements of structural carbohydrates were analyzed using the Microsoft Excel "TTEST" formula which uses the Student's t-test. The test was run using two tails, assuming equal variance. Significance was measured at $\alpha = 0.05$ and 0.10 for each dataset. If the results were the same at both alpha levels, only the lowest alpha level was displayed on the corresponding figure.

## 2.17 Interpretation of data

The results that make up the majority of the discussion chapter were chosen based on a combination of strong trends and statistical significance. A strong trend was defined as a characteristic that was seen in all the lines examined for a particular construct, but one that was not necessarily statistically significant for all of the aforementioned lines. For example, if all four lines showed an increasing trend in crystallinity, but only one line showed a statistically significant increase, this would be considered a strong trend and would make up part of the discussion. Conversely, if two of five lines showed a statistically significant increase in crystallinity, but the remaining three lines showed a decreasing trend, this result would not be discussed and deemed inconclusive. In this manner, the results relevant to the discussion chapter were chosen.

# Chapter 3: Results

## 3.1 Identification of Arabidopsis and poplar orthologs by phylogenetic analysis of glycosyl hydrolase family 9

In order to identify the correct poplar and Arabidopsis orthologs from the poplar transcriptome data, a neighbour-joining phylogenetic tree (1000 bootstrap) was constructed combining the GH9 family of both species (Figure 3.1). The outgroup used to root the tree was *Selaginella moellendorffii* (XP_002985347). This phylogenetic tree confirmed that POPTR_0005s25890 (PtGH9B5) was most similar to At1g19940 (AtGH9B5) and POPTR_0003s13940 (PtGH9C2) was most similar to At1g64390 (AtGH9C2). Therefore, these genes were chosen for examination in this study. Additionally, this tree identified other orthologous Arabidopsis and poplar endoglucanases which may be of interest to future researchers.

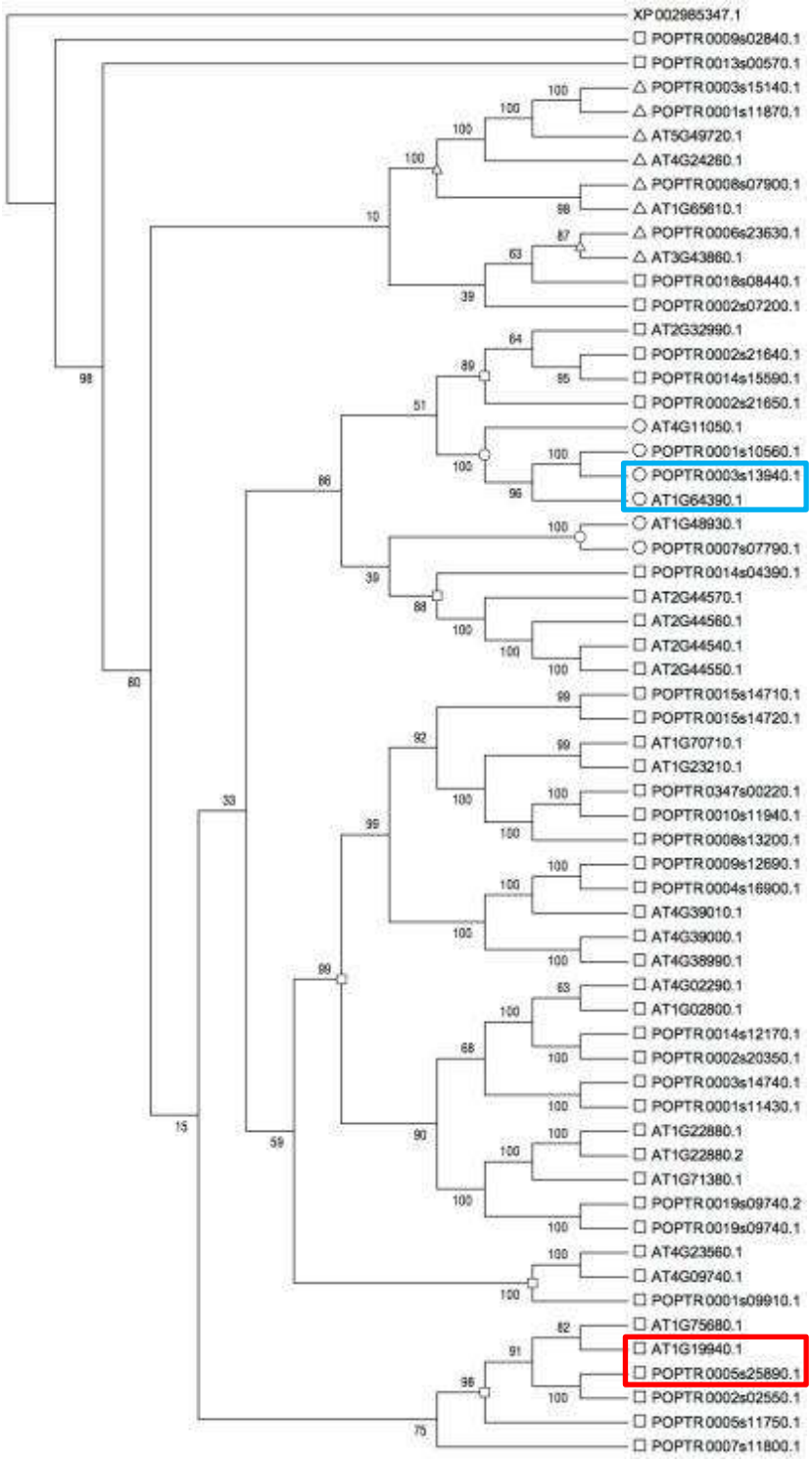


Figure 3.1. Phylogenetic tree of Arabidopsis and poplar GH9 family members.
Red outline = AtGH9B5/PtGH9B5 orthologs, blue outline = AtGH9C2/PtGH9C2 orthologs.
Shapes denote endoglucanase class: triangles = Class A; squares = Class B; circles = Class C.

## 3.2 Plant growth and microscopy of Arabidopsis t-DNA insertion mutants

A mutant t-DNA insertion seed line for each endoglucanase gene was obtained from the Arabidopsis Biological Resource Centre. The t-DNA insertion line SALK_121501 contains a t-DNA insertion in the promoter region of AtGH9B5, while line CS25087 contains a t-DNA insertion in an exon of AtGH9C2. Mutants were confirmed for homozygosity of the t-DNA insertion prior to analysis. Plant growth was similar in appearance to wild-type Arabidopsis plants grown concurrently. Stem cross-sections were taken approximately 1 cm from the base of the plant, stained with toluidine blue, and were then examined under a light microscope on a weekly basis beginning at approximately 28 DAG. No apparent differences in the arrangement or structure of cells compared to wild-type were apparent (Figure 3.2, Figure 3.3).

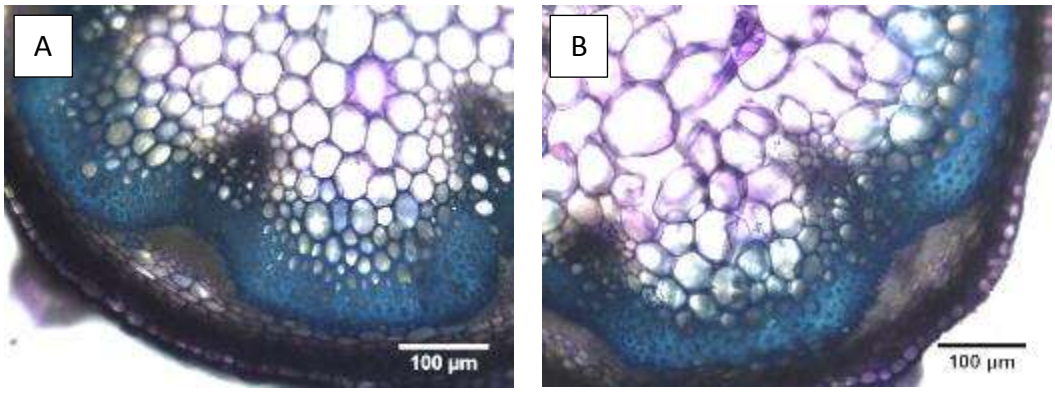


Figure 3.2. Toluidine blue stained stem cross-sections of a) wild-type, and b) *atgh9b5*.

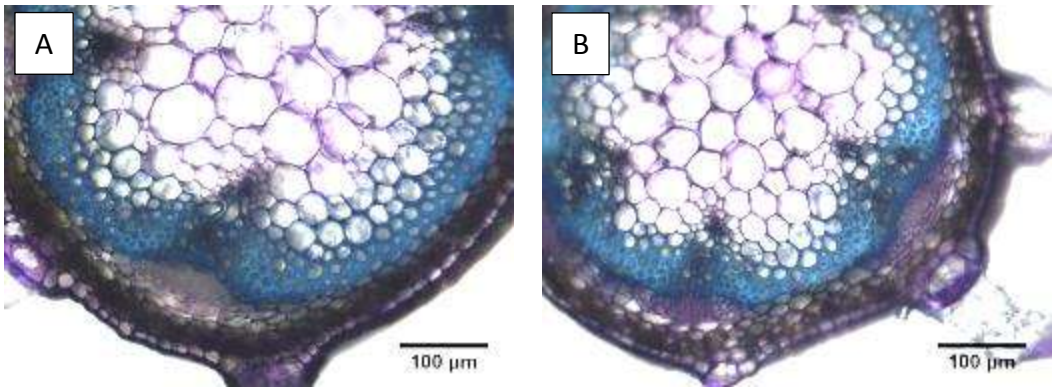


Figure 3.3. Toluidine blue stained stem cross-sections of a) wild-type and b) *atgh9c2*.

## 3.3 Cell wall crystallinity and microfibril angle

In order to assess cell wall ultrastructure, the crystallinity of each of the t-DNA mutant lines was measured at the base of 8-week old stem segments. Both mutants showed an increase in crystallinity compared to wild-type, with the *atgh9b5* mutant showing a 4% increase (statistically significant at $\alpha = 0.10$ but not $\alpha = 0.05$, Figure 3.4), while the *atgh9c2* mutant showed a 2.4% increase (not statistically significant at $\alpha = 0.05$, Figure 3.5).

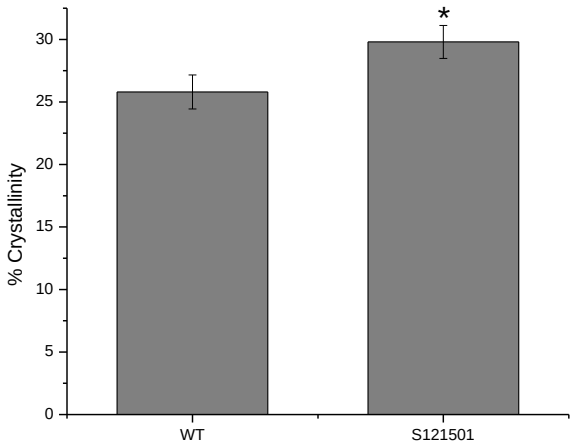


Figure 3.4. Cell wall crystallinity of wild-type and *atgh9b5* plant stems. Asterisk indicates a significant difference measured using a Student's t-test at $\alpha = 0.10$ (n=5).

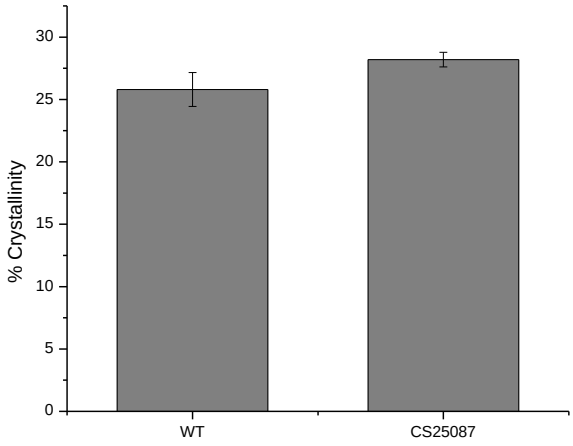


Figure 3.5. Cell wall crystallinity of wild-type and *atgh9c2* plant stems. No significant difference measured using a Student's t-test at $\alpha = 0.05$ (n=5).

## 3.4 Structural carbohydrate analysis

The percentage variation in cell wall polysaccharides was measured using a micro-Klason analysis, and quantified by HPLC. The monomeric carbohydrates measured included arabinose, rhamnose, galactose, glucose, xylose, and mannose. The *atgh9b5* stem cell walls had slight decreases in each carbohydrate, with glucose decreasing by an average of 1.3% (Table 3.1). In contrast, the *atgh9c2* stems did not show a similar trend, as composition of both arabinose and xylose was higher than the wild-type plants, which may reflect an overall increase in arabinoxylan (Table 3.1). Mannose was similar, while rhamnose and galactose decreased. In addition, consistent with the *atgh9b5* mutant stems, there was a decrease in total cell wall glucose content.

Table 3.1. Percentage of sugar per mass of sample in t-DNA insertion lines. Bold values indicate a significant difference measured using a Student's t-test at $\alpha = 0.10$, while underlined values indicate a significant difference at $\alpha = 0.05$ (n=3).

| | Arabinose | Rhamnose | Galactose | Glucose | Xylose | Mannose |
|---|---|---|---|---|---|---|
| **WT** | 1.55 (0.14) | 1.43 (0.28) | 2.61 (0.17) | 34.16 (0.57) | 12.16 (0.37) | 2.12 (0.11) |
| **atgh9b5** | 1.46 (0.07) | 1.33 (0.05) | 2.24 (0.02) | 33.24 (0.52) | 11.74 (0.95) | 1.93 (0.06) |
| **atgh9c2** | 1.61 (0.11) | 1.14 (0.03) | 2.34 (0.15) | 32.55 (0.93) | 13.08 (0.43) | 2.19 (0.29) |

## 3.5 Visualization of AtGH9B5 and AtGH9C2 promoter activity utilizing YFP in Arabidopsis

In order to localize promoter activity, AtGH9B5pr::YFP and AtGH9C2pr::YFP constructs were made. Agrobacterium-mediated transient expression was performed on 4-day old Arabidopsis seedlings. After two days of co-cultivation with Agrobacterium, seedlings were viewed using fluorescence microscopy. Both constructs resulted in a clear YFP signal in the young seedlings, particularly along the top end of the petiole and sometimes extending into the cotyledons (Figure 3.6, Figure 3.7).

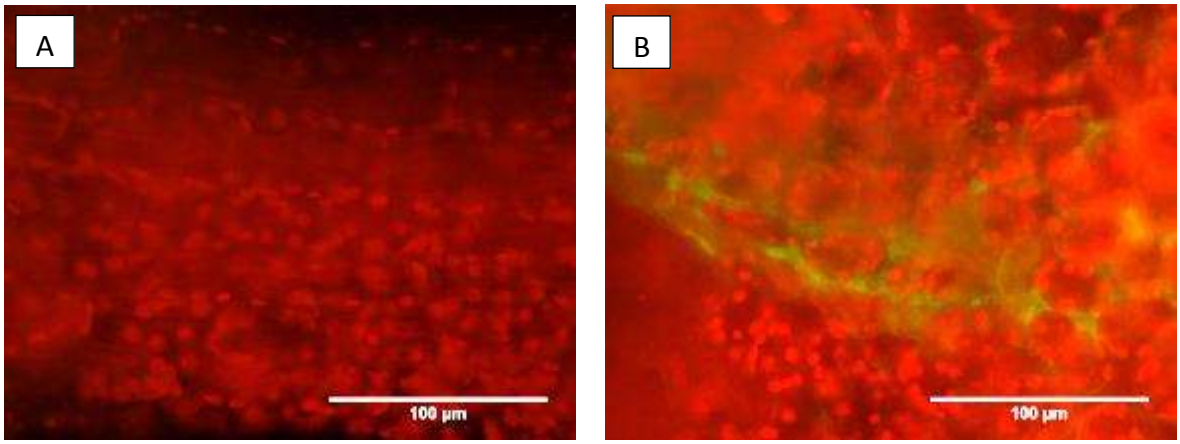


Figure 3.6. Transient expression of AtGH9B5pr::YFP in 6-day old Arabidopsis seedlings in a) control, and b) transformants. Images represent top of petiole to base of cotyledon.

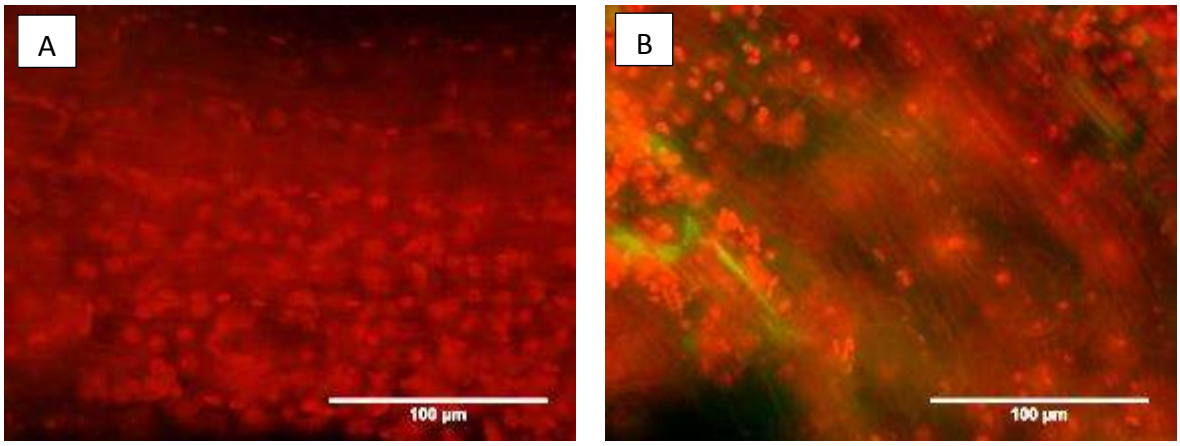


Figure 3.7. Transient expression of AtGH9C2pr::YFP in 6-day old Arabidopsis seedlings in a) control, and b) transformants. Images represent the petiole.

Stable transformants of the same constructs were also created by spraying flowers of maturing wild-type Arabidopsis plants with Agrobacterium containing the AtGH9B5pr::YFP and AtGH9C2pr::YFP constructs, respectively. The T1 seeds were planted, and potential transformants screened for the presence of YFP using PCR, before being viewed under the microscope. The root, hypocotyl, and cotyledons of PCR positive T2 seedlings were viewed using fluorescence and/or confocal microscopy beginning at 4 days after germination (DAG).

In the AtGH9B5pr::YFP transgenic plants (confirmed transgenic by PCR), no YFP signal was seen in any of the tissues examined, or at any of the time points screened (4, 6, 8, 11, 35, and 49 DAG). Once the plants had bolted, stem cross-sections were also examined under the microscope, but again no signal was visible. The AtGH9C2pr::YFP stable transformants were also viewed beginning at 4 DAG. At this developmental stage, YFP signal was noticed in the hypocotyl parenchyma in the form of punctae which tended to associate with the edge of the cell, particularly at the top and bottom (Figure 3.8). YFP punctae were also clearly visible in the cotyledon leaf parenchyma (Figure 3.8). The stable transformants were examined again at 6, 8, and 11 DAG. At these latter time points, the YFP punctae were still clearly visible in the hypocotyl parenchyma, though not with the same frequency. In contrast, the signal in the cotyledon parenchyma was no longer visible. No signal was observed at any time point in the roots and true leaves. Additionally, no expression was seen in the developing vascular cylinder of the stem or root.

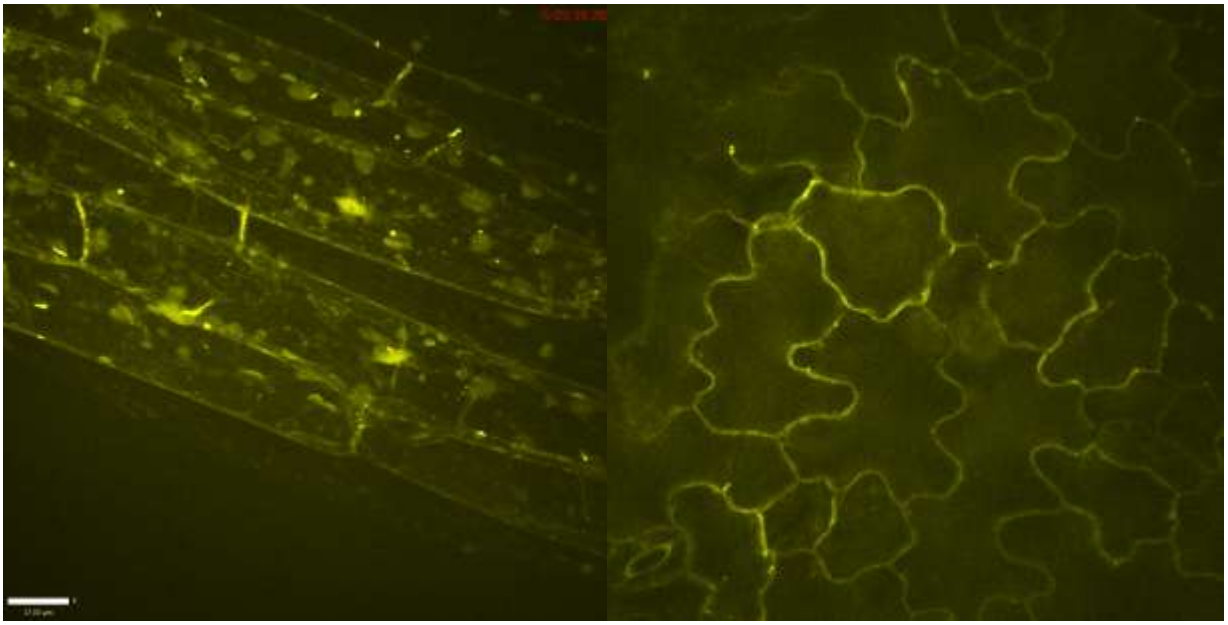

Figure 3.8. Hypocotyl (left) and cotyledon (right) of stable Arabidopsis AtGH9C2pr::YFP transformants.

## 3.6 35S::PtGH9B5 and 35S::PtGH9C2 over-expression in Arabidopsis

### 3.6.1 Plant growth and microscopy

Seeds were collected from several independently transformed plants which had previously been determined to be positive for the 35S::PtGH9B5 and/or 35S::PtGH9C2 constructs, respectively. Each set of seeds was planted and analyzed separately to give rise to four independent lines for the 35S::PtGH9B5 construct and five lines for the 35S::PtGH9C2 construct. The height of the plants was measured based on the main stem at 8-weeks of age, and shown not to be different compared to wild-type for any of the 35S overexpression plant lines (Figure 3.9, Figure 3.10).

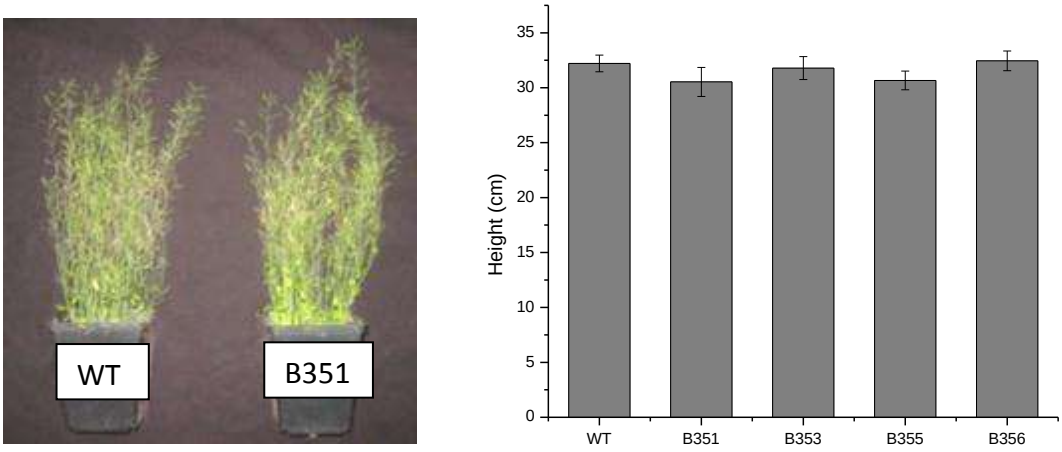


Figure 3.9. Growth (left) and average heights (right) of wild-type and 35s::PtGH9B5 plant lines. No significant difference was measured using a Student's t-test at α = 0.05 or 0.10 (n=20).

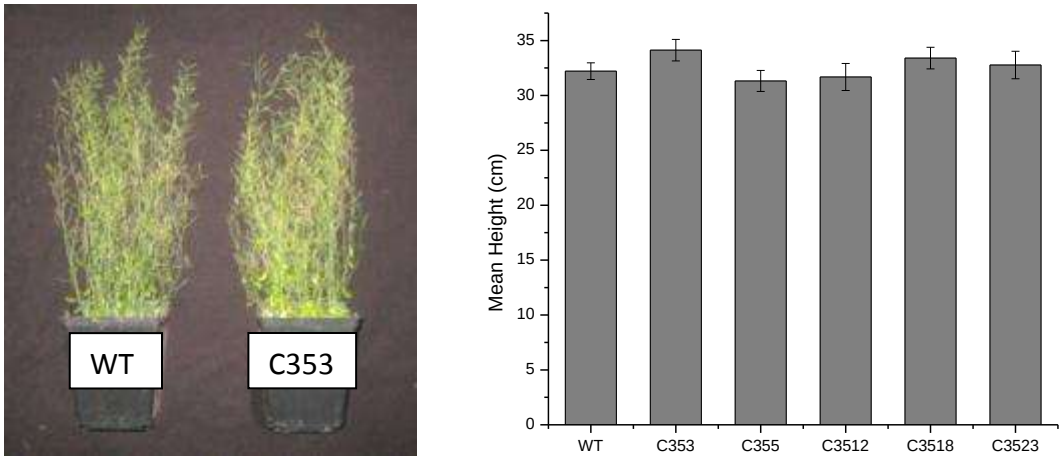


Figure 3.10. Growth (left) and average heights (right) of wild-type and 35S::PtGH9C2 plant lines. No significant difference was measured using a Student's t-test at α = 0.05 or 0.10 (n=20).

In order to determine if any changes had taken place on the cellular level, cross-sections from the base of the plant stems were stained with toluidine blue and examined microscopically on a weekly basis beginning at approximately 28 DAG. There were no apparent differences in cell patterning, shape, or size compared to wild-type (Figure 3.11, Figure 3.12).

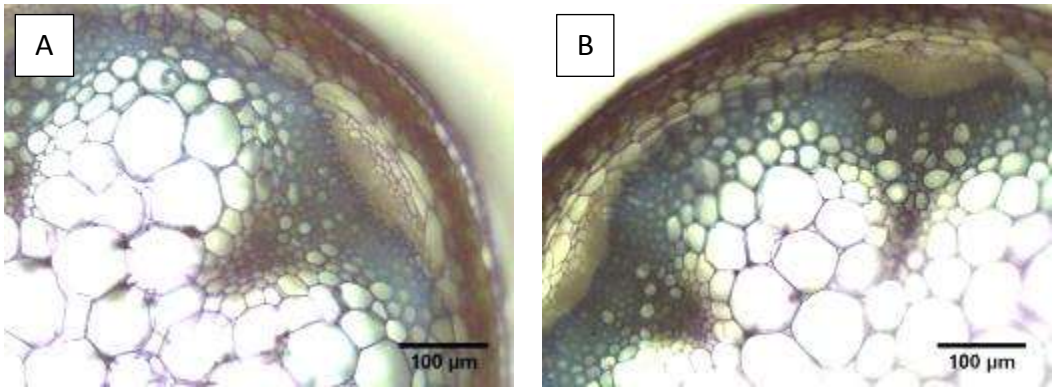


Figure 3.11. Toluidine blue stained stem cross-sections of a) wild-type, and b) B354.

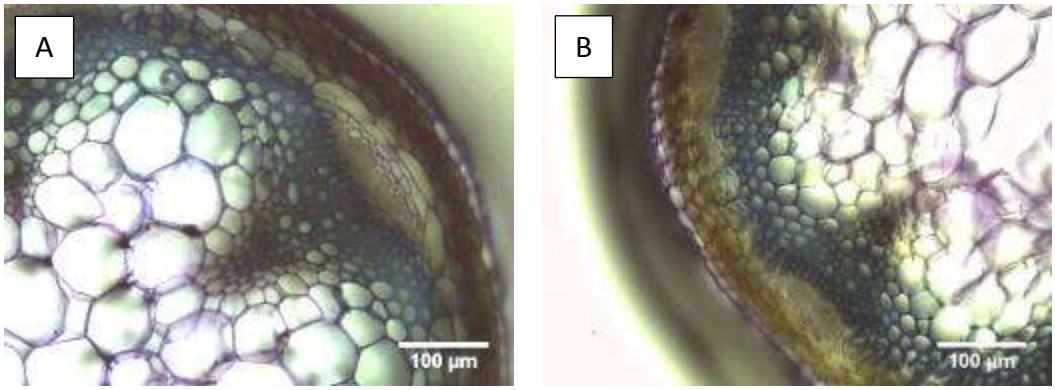


Figure 3.12. Toluidine blue stained stem cross-sections of a) wild-type, and b) C353.

### 3.6.2 Relative expression of PtGH9B5 and PtGH9C2 in Arabidopsis 35S over-expression constructs

Quantitative PCR was used to determine the level of expression of the poplar gene in each plant line. The expression of the transgene was calculated relative to the expression of the reference gene EF1α for each sample. All 35S::PtGH9B5 lines had confirmed expression of the poplar gene with lines B353 and B355 showing relatively higher transcript abundance compared to the other lines (Figure 3.13). Similarly, all 35S::PtGH9C2 lines showed expression of PtGH9C2 in Arabidopsis, with line C3523 exhibiting approximately twice the relative expression of the other lines (Figure 3.14).

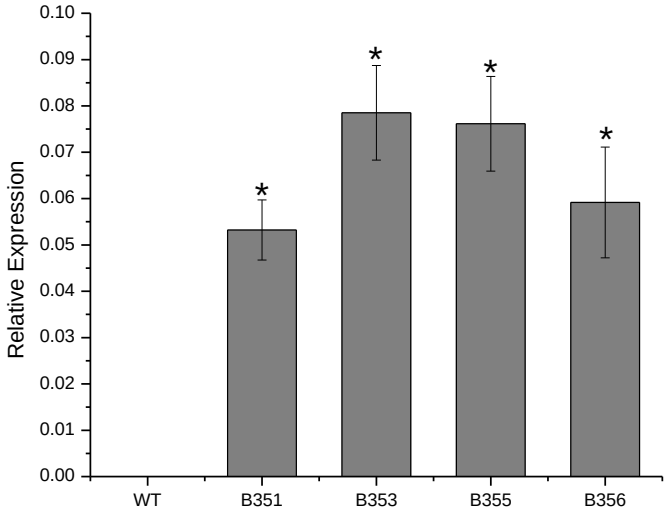


Figure 3.13. Relative expression of PtGH9B5 in wild-type and 35S::PtGH9B5 plant lines. Asterisks indicate a significant difference measured using a Student's t-test at α = 0.05 (n=3).

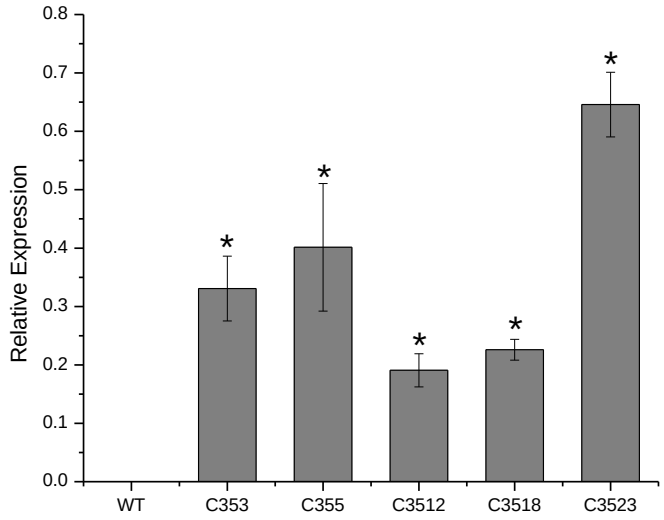


Figure 3.14. Relative expression of PtGH9C2 in wild-type and 35S::PtGH9C2 plant lines. Asterisks indicate a significant difference measured using a Student's t-test at α = 0.05 (n=3).

### 3.6.3 Cell wall crystallinity and microfibril angle

In order to determine if there were any changes in cell wall ultrastructure, cell wall crystallinity and microfibril angle were measured using X-ray diffraction on dried 8-week old stems. The 35S::PtGH9B5 plants showed a decreasing trend in crystallinity, particularly in lines B351, B353, and B355 which showed an average decrease of 3.9% (Figure 3.15). Microfibril angle was not

different compared to wild-type plants (Figure 3.15). The 35S::PtGH9C2 plant lines displayed no clear trends in crystallinity compared to wild-type (Figure 3.16). Lines C3512 and C3518 show a decrease in crystallinity, while C353 and C3523 were similar to wild-type, and C355 shows an increase in crystallinity. Conversely, the trend in MFA is more clear, as lines C3512, C3518, and C3523 have on average a 2.2 degree larger MFA compared to wild-type (Figure 3.16).

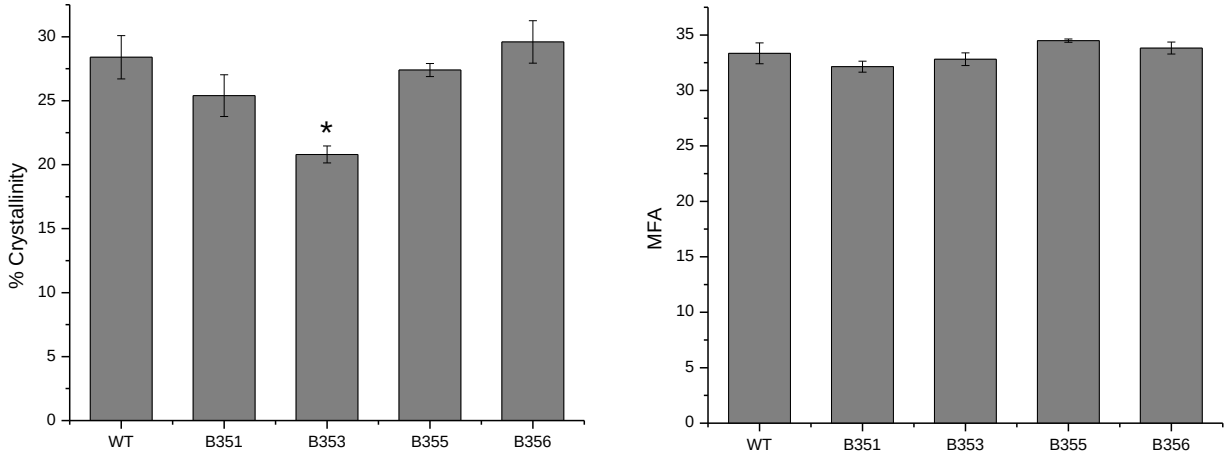


Figure 3.15. Cell wall crystallinity and MFA of wild-type and 35S::PtGH9B5 plant stems. Asterisks indicate a significant difference measured using a Student's t-test at α = 0.05 (n=5).

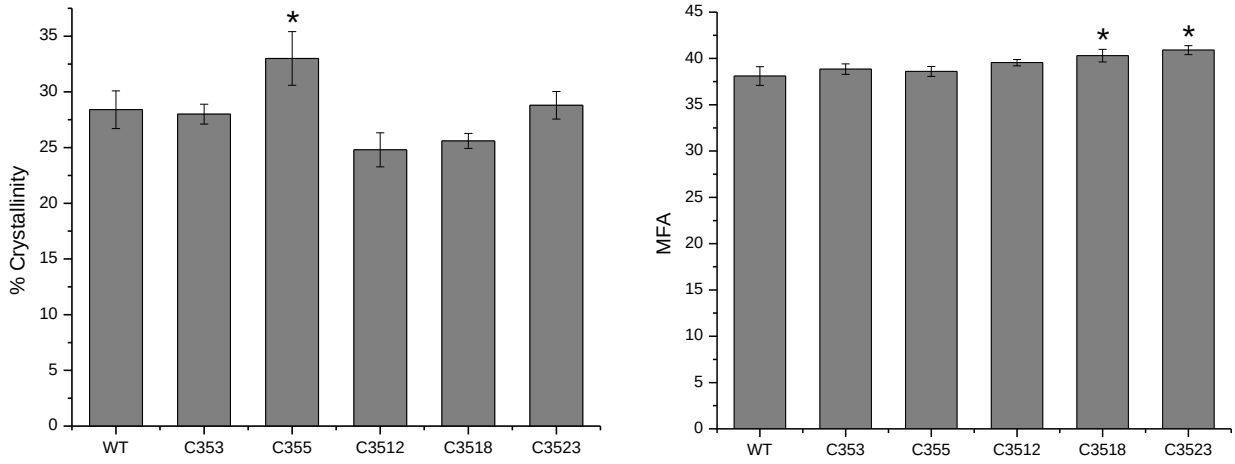


Figure 3.16. Cell wall crystallinity and MFA of wild-type and 35S::PtGH9C2 plant stems. Asterisks indicate a significant difference measured using a Student's t-test at α = 0.05 (n=5).

### 3.6.4 Structural carbohydrate analysis

The percentage cell wall polysaccharides were again determined and compared to the composition of wild-type plants. The 35S::PtGH9B5 plant lines, showed a decrease in rhamnose, glucose, and xylose in all lines, except B355. The decrease in rhamnose ranged from 4.4-22.4%, while glucose decreased by 0.9-4.7%, and the decrease in xylose ranged from 2.7-11.7% (Table 3.2). In the 35S::PtGH9C2 transgenic plants, there was a similar trend in lines C353, C3512, and C3523, all of which showed a decrease in xylose and glucose. In these lines, xylose decreased by 2.0-20.3% while glucose decreased by 2.0-7.9% (Table 3.3). Additionally, lines C355, C3512, and C3518 showed an average increase in galactose of 11.4±1.1%.

Table 3.2. Percentage of sugar per mass sample in 35S::PtGH9B5 plant lines. Bold values indicate a significant difference measured using a Student's t-test at $\alpha = 0.10$, while underlined values indicate a significant difference at $\alpha = 0.05$ (n=3).

| | Arabinose | Rhamnose | Galactose | Glucose | Xylose | Mannose |
|---|---|---|---|---|---|---|
| **WT** | 0.78 (0.02) | 0.92 (0.10) | 1.48 (0.01) | 28.91 (0.64) | 12.67 (0.79) | 1.56 (0.09) |
| **B351** | 0.82 (0.04) | 0.71 (0.08) | 1.45 (0.03) | 27.55 (0.17) | 11.18 (0.19) | 1.62 (0.23) |
| **B353** | 0.76 (0.04) | 0.88 (0.10) | 1.47 (0.03) | 28.66 (0.75) | 11.95 (0.82) | 1.58 (0.05) |
| **B355** | 0.78 (0.02) | 0.97 (0.04) | **1.55 (0.02)** | **32.27 (0.83)** | 14.02 (0.22) | 1.73 (0.00) |
| **B356** | 0.80 (0.02) | 0.78 (0.12) | 1.53 (0.06) | 28.53 (0.65) | 12.32 (0.28) | 1.84 (0.14) |

Table 3.3. Percentage of sugar per mass sample in 35S::PtGH9C2 plant lines. Bold values indicate a significant difference measured using a Student's t-test at $\alpha = 0.10$, while underlined values indicate a significant difference at $\alpha = 0.05$ (n=3).

| | Arabinose | Rhamnose | Galactose | Glucose | Xylose | Mannose |
|---|---|---|---|---|---|---|
| **WT** | 0.77 (0.03) | 1.09 (0.06) | 1.53 (0.06) | 29.46 (0.62) | 10.61 (0.67) | 1.76 (0.06) |
| **C353** | 0.73 (0.05) | 1.08 (0.05) | 1.51 (0.12) | **27.14 (0.45)** | 9.19 (0.66) | **1.56 (0.04)** |
| **C355** | 0.83 (0.04) | 1.18 (0.05) | 1.74 (0.12) | 30.98 (0.54) | 11.75 (0.56) | 1.81 (0.06) |
| **C3512** | 0.85 (0.02) | **1.34 (0.04)** | 1.82 (0.14) | 29.49 (0.62) | 9.72 (1.39) | 1.77 (0.06) |
| **C3518** | **0.88 (0.02)** | 1.14 (0.03) | **1.68 (0.03)** | 30.07 (0.60) | 11.22 (0.31) | 1.78 (0.03) |
| **C3523** | 0.72 (0.06) | 0.95 (0.02) | 1.43 (0.05) | 27.67 (0.77) | 8.73 (1.01) | 1.57 (0.05) |

## 3.7 AtCesA8pr::PtGH9B5 and AtCesA8pr::PtGH9C2 over-expression in Arabidopsis

### 3.7.1 Plant growth and microscopy

The Arabidopsis CesA8 promoter was used to induce expression of each poplar gene respectively, during secondary cell wall development in Arabidopsis. Seeds were collected from four separate plants which had previously been determined to be positive for the expression of AtCesA8pr::PtGH9B5 and/or AtCesA8pr::PtGH9C2 constructs, respectively. Each set of seeds was planted and analyzed separately to give rise to four plant lines. The height of the plants was measured from the base of the 8-week old stem to the top of the plant (Figure 3.17, Figure 3.19). Rosette diameters were also measured at their widest diameter, before the plants bolted, at 21 DAG (Figure 3.17, Figure 3.19). There was an average decrease in height of 2.4cm in the AtCesA8pr::PtGH9B5 plant lines (5.1 %), as well as an average decrease of 14.8mm in rosette diameter (33.1 %)(Figure 3.18). The AtCesA8pr::PtGH9C2 plant lines demonstrated a similar trend. Height was reduced in all plant lines by an average of 3.8cm (11.1%), while rosette diameter was smaller in width by an average of 14.5mm (31.4 %, Figure 3.20).

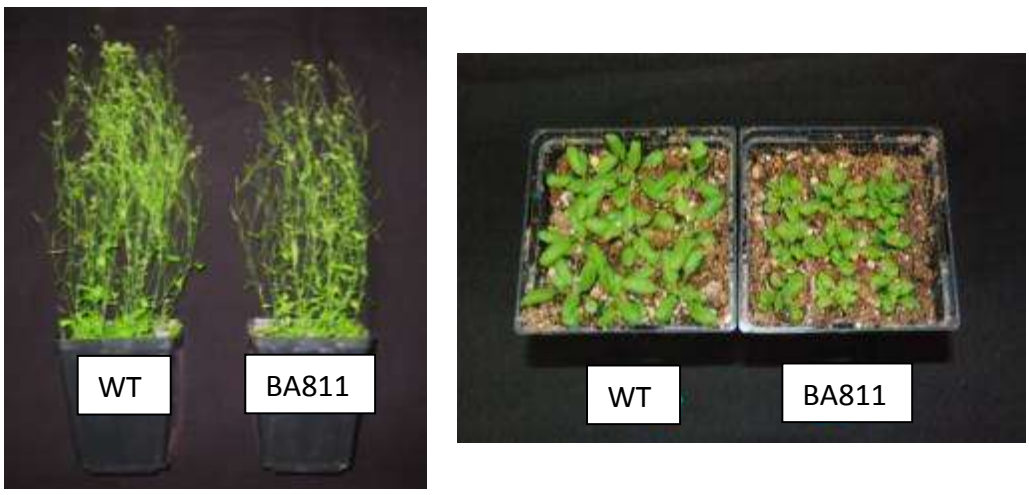


Figure 3.17. Growth of wild-type and AtCesA8pr::PtGH9B5 plants.

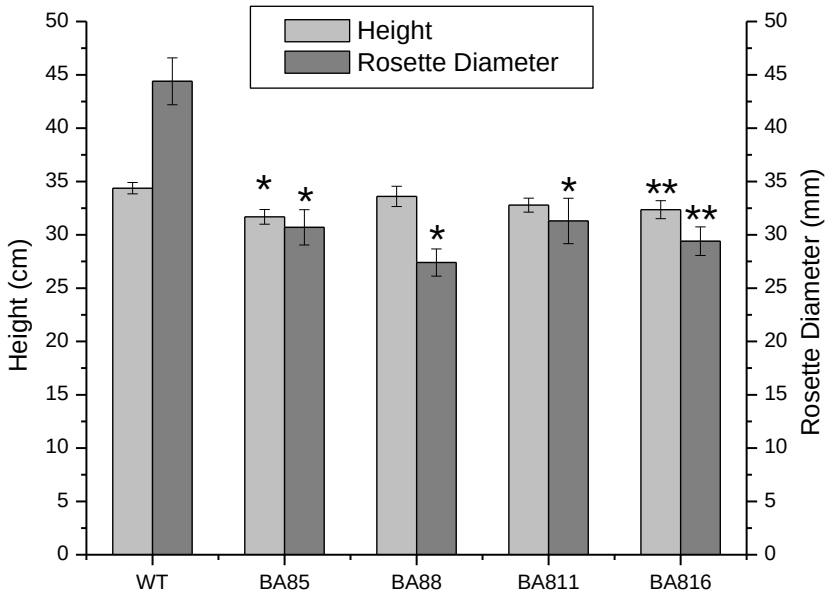


Figure 3.18. Height (n=20) and maximum rosette diameter (n=10) of wild-type and AtCesA8pr::PtGH9B5 plants. (*) significant at α = 0.05; (**) significant at α = 0.10, measured using a Student's t-test.

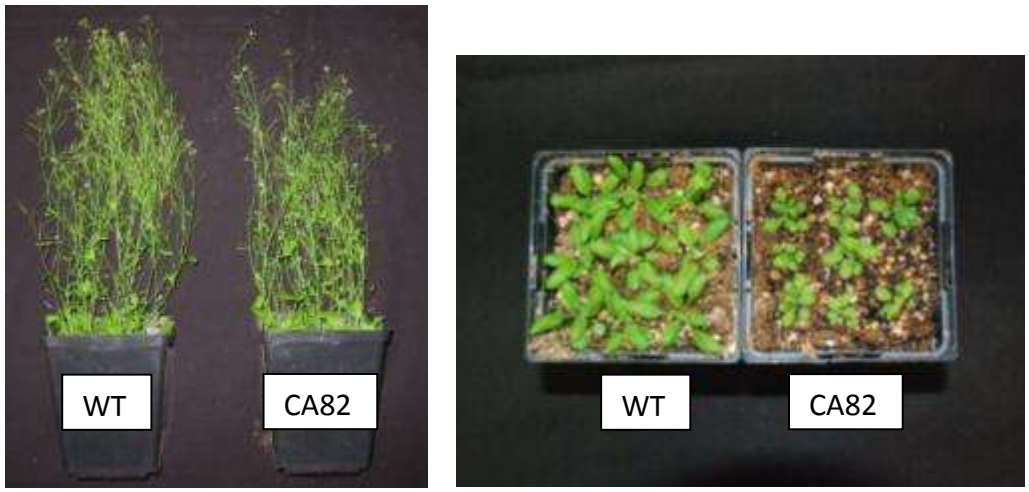


Figure 3.19. Growth of wild-type and AtCesA8pr::PtGH9C2 plants.

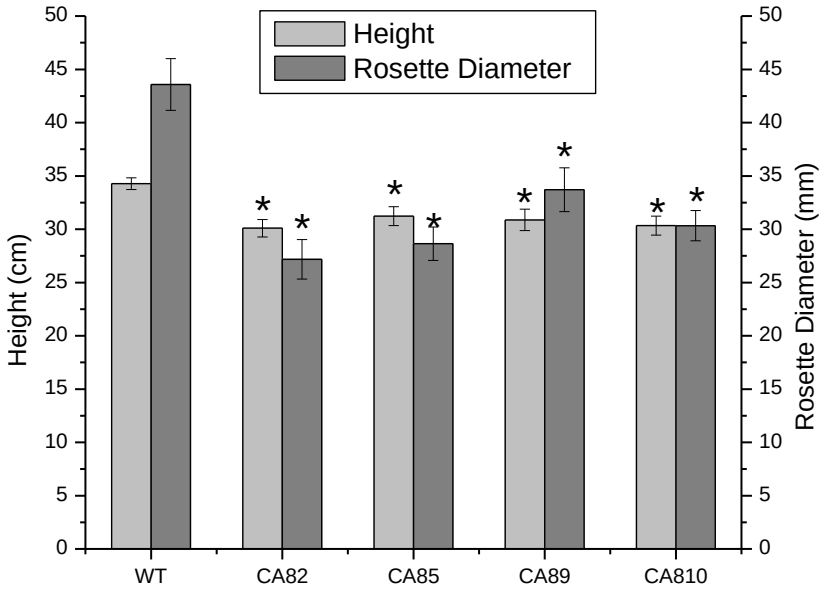


Figure 3.20. Height (n=20) and maximum rosette diameter (n=10) of wild-type and AtCesA8pr::PtGH9C2 plants. Asterisks indicate a significant difference measured using a Student's t-test at $\alpha = 0.05$.

In order to further investigate possible reasons for the stunted growth phenotype, stem cross-sections of each plant line were examined on a weekly basis, beginning at approximately 28 DAG, for changes in cell patterning, size, and shape. Sections were stained with toluidine blue and examined using light microscopy. Again, there were no apparent changes in cell morphology compared to wild-type in any of the transgenic plant lines (Figure 3.21, Figure 3.22).

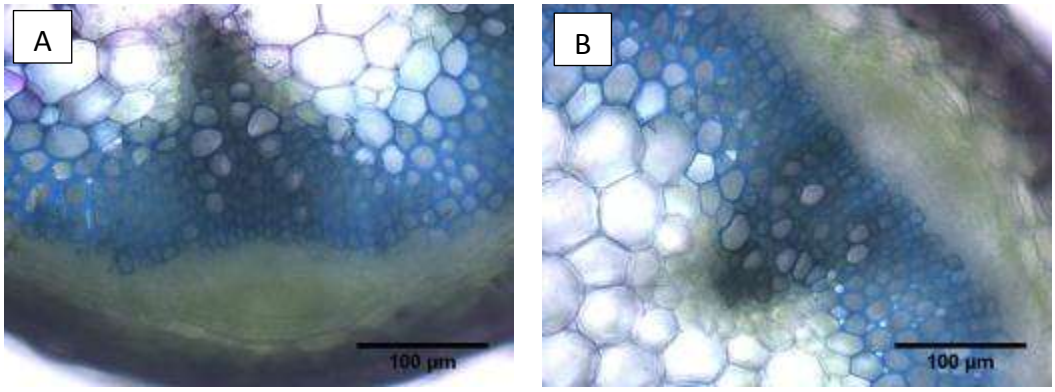


Figure 3.21. Toluidine blue stained stem cross-sections of a) wild-type, and b) AtCesA8pr::PtGH9B5 plants.

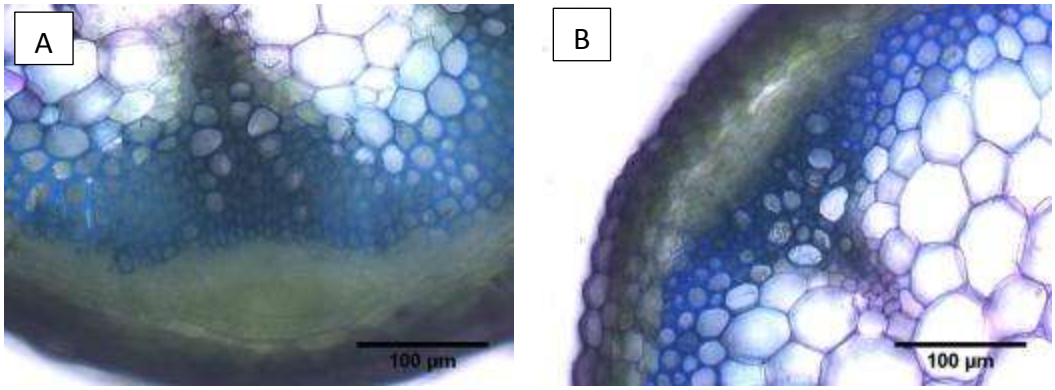


Figure 3.22. Toluidine blue stained stem cross-sections of a) wild-type, and b) AtCesA8pr::PtGH9C2 plants.

### 3.7.2 Relative expression of PtGH9B5 and PtGH9C2 in AtCesA8pr over-expression constructs in Arabidopsis

Quantitative PCR was used to determine if the respective poplar genes were being expressed in Arabidopsis stem tissue. Each transgenic line was tested and confirmed for the presence of the PtGH9B5 and/or PtGH9C2 transcript. Relative expression levels were calculated based on the expression of the reference gene, EF1α, in each sample. The AtCesA8pr::PtGH9B5 plant lines with particularly high expression of the poplar gene included BA85, BA88, and BA816 (Figure 3.23). Line BA811 only had low levels of PtGH9B5expression. Similarly, all AtCesA8pr::PtGH9C2

plant lines confirmed expression of PtGH9C2 (Figure 3.24). Line CA810 showed the highest level of expression of the poplar gene while CA812 had the lowest, and the remaining lines were similar in their levels of expression.

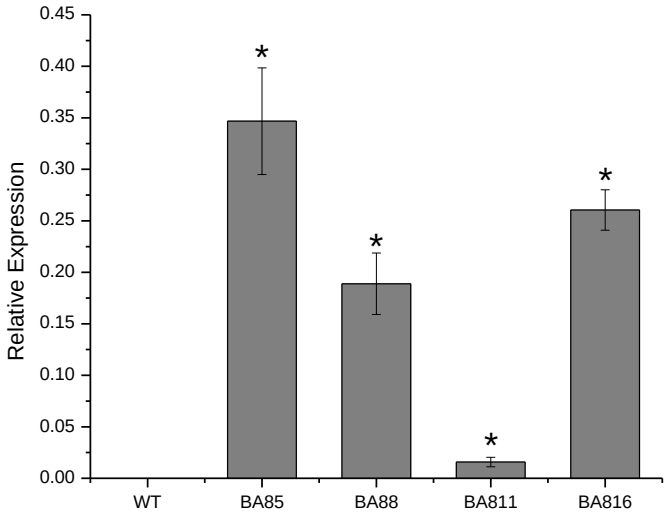


Figure 3.23. Relative expression of PtGH9B5 in wild-type and AtCesA8pr::PtGH9B5 plant lines. Asterisks indicate a significant difference measured using a Student's t-test at α = 0.05 (n=3).

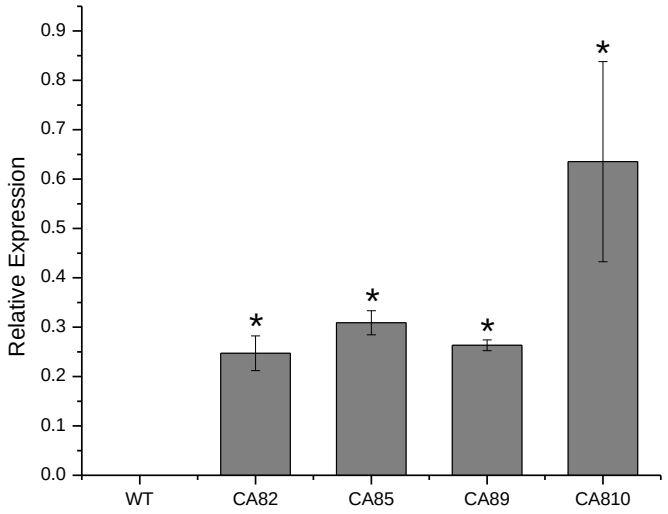


Figure 3.24. Relative expression of PtGH9C2 in wild-type and AtCesA8pr::PtGH9C2 plant lines. Asterisks indicate a significant difference measured using a Student's t-test at α = 0.05 (n=3).

### 3.7.3 Cell wall crystallinity and microfibril angle

In order to assess if there were any changes in cell wall ultrastructure in the transgenic plant lines, X-ray diffraction was used to estimate cell wall crystallinity and MFA. For the AtCesA8pr::PtGH9B5 plants, crystallinity measurements displayed an increasing trend compared to wild-type (Figure 3.25). Lines BA85, BA811, and BA816 showed an average increase of 2.1% in crystallinity, while MFA was not altered compared to wild-type (Figure 3.25). In the AtCesA8pr::PtGH9C2 plant lines, cell wall crystallinity showed an average increase of 3.7%, with CA82 showing the most significant increase (6.8%; $\alpha = 0.05$)(Figure 3.26). MFA also showed an increasing trend compared to wild-type, with lines CA85 and CA810 showing the greatest increase (~ 1.5 degrees)(Figure 3.26).

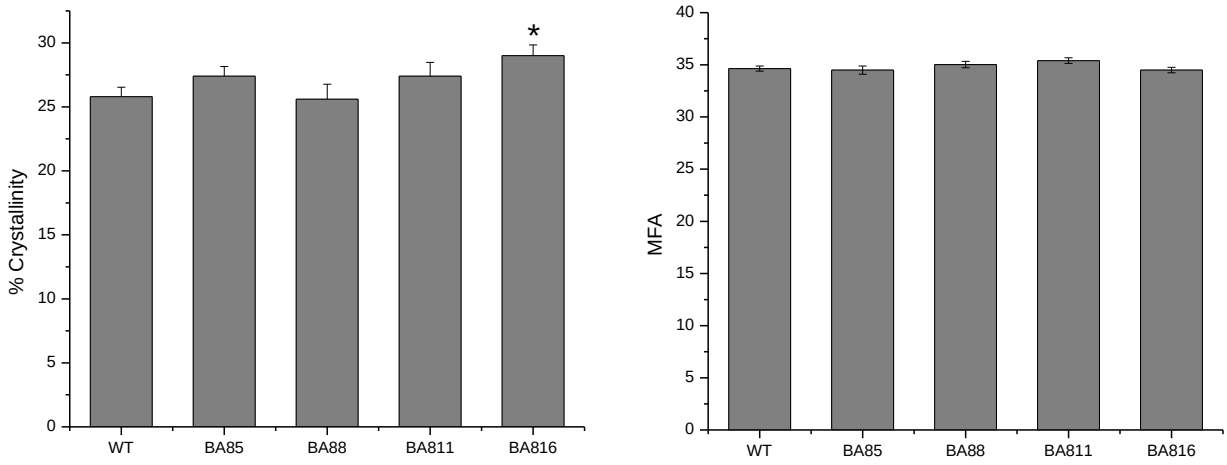


Figure 3.25. Cell wall crystallinity and MFA of wild-type and AtCesA8pr::PtGH9B5 plant stems. Asterisks indicate a significant difference measured using a Student's t-test at $\alpha = 0.05$ (n=5).

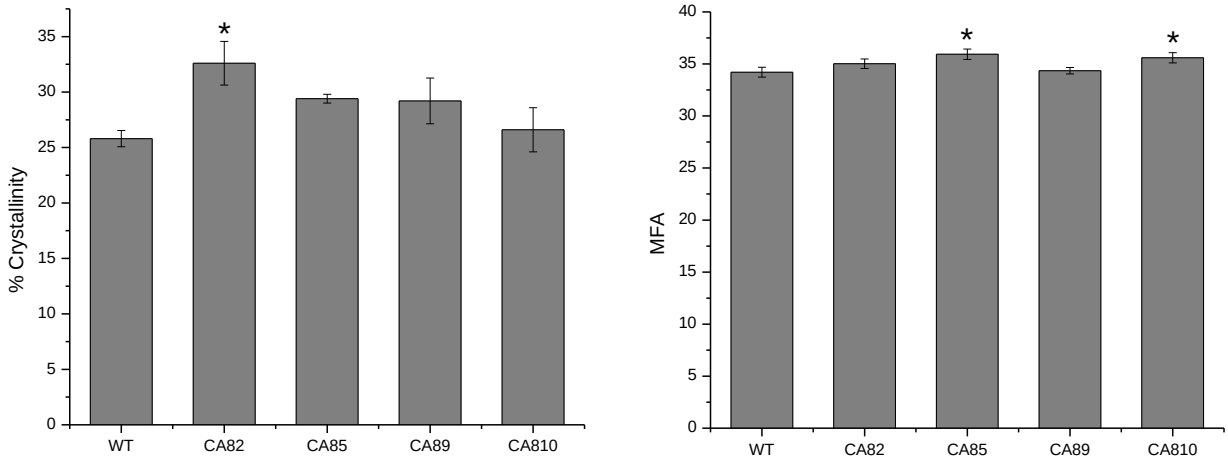


Figure 3.26. Cell wall crystallinity and MFA of wild-type and AtCesA8pr::PtGH9C2 plant stems. Asterisks indicate a significant difference measured using a Student's t-test at $\alpha = 0.05$ (n=5).

### 3.7.4 Structural carbohydrate analysis

Cell wall chemical analysis showed that all AtCesA8pr::PtGH9B5 plant lines had an increasing trend in arabinose, galactose, glucose, and xylose (Table 3.4). Arabinose and galactose showed a similar average increase of 11.5±3.3% and 11.5±3.7%, respectively across all plant lines. Glucose increased by 14.0±2.8% on average, while xylose increased the greatest average amount (18.0±3.8%). Measurements of AtCesA8pr::PtGH9C2 stems demonstrated that all lines had less arabinose, rhamnose, xylose, and mannose (Table 3.5). CA89 and CA810 showed the greatest differences compared to wild-type, which included a decrease in glucose of 3.5% and 10.4%, a decrease in xylose of 12.7% and 16.7%, and a decrease in galactose of 3.7% and 8.4%, respectively.

Table 3.4. Percentage of sugar per mass sample in AtCesA8pr::PtGH9B5 plant lines. Bold values indicate a significant difference measured using a Student's t-test at α = 0.10, while underlined values indicate a significant difference at α = 0.05 (n=3).

| | Arabinose | Rhamnose | Galactose | Glucose | Xylose | Mannose |
|---|---|---|---|---|---|---|
| **WT** | 0.76 (0.02) | 0.93 (0.11) | 1.57 (0.03) | 25.39 (0.41) | 9.04 (0.47) | 1.49 (0.02) |
| **BA85** | 0.78 (0.03) | 0.91 (0.10) | 1.64 (0.04) | **28.23 (0.38)** | **10.19 (0.21)** | **1.64 (0.06)** |
| **BA88** | **0.86 (0.01)** | 0.85 (0.07) | **1.80 (0.02)** | **29.72 (0.43)** | **10.89 (0.27)** | 1.61 (0.05) |
| **BA811** | **0.87 (0.01)** | 0.99 (0.08) | **1.86 (0.05)** | **30.25 (0.46)** | **11.40 (0.29)** | **1.79 (0.04)** |
| **BA816** | 0.86 (0.11) | 0.83 (0.03) | 1.69 (0.13) | 27.57 (1.57) | 10.18 (0.67) | 1.66 (0.13) |

Table 3.5. Percentage of sugar per mass sample in AtCesA8pr::PtGH9C2 plant lines. Bold values indicate a significant difference measured using a Student's t-test at α = 0.10, while underlined values indicate a significant difference at α = 0.05 (n=3).

| | Arabinose | Rhamnose | Galactose | Glucose | Xylose | Mannose |
|---|---|---|---|---|---|---|
| **WT** | 0.76 (0.04) | 0.78 (0.17) | 1.51 (0.02) | 25.63 (0.40) | 8.66 (0.23) | 1.41 (0.01) |
| **CA82** | 0.73 (0.01) | 0.64 (0.10) | 1.52 (0.02) | 25.89 (0.23) | 8.64 (0.06) | 1.41 (0.00) |
| **CA85** | 0.72 (0.02) | 0.76 (0.11) | 1.54 (0.01) | 25.89 (0.43) | 8.36 (0.26) | 1.34 (0.03) |
| **CA89** | **0.61 (0.01)** | 0.67 (0.06) | 1.45 (0.02) | 24.74 (0.17) | **7.56 (0.05)** | **1.33 (0.01)** |
| **CA810** | **0.59 (0.03)** | 0.74 (0.04) | **1.38 (0.00)** | 22.97 (0.71) | 7.21 (0.56) | **1.17 (0.04)** |

## 3.8 RNAi down-regulation of AtGH9C2 in Arabidopsis

### 3.8.1 Plant growth and microscopy

Seeds were collected from three separate plants which had previously been determined to be positive for the RNAi::AtGH9C2 construct. Each set of seeds was planted and analyzed separately to give rise to three plant lines. The height of the plants was measured based on the main stem at 8-weeks of age, while the rosette diameter was measured at 34 DAG at the widest part of the rosette (Figure 3.27). Plant height showed an increase compared to wild-type, with an average increase of 1.1cm (3.3%), while rosette diameter also showed an increasing trend by as much as 10mm in line R10 (22%)(Figure 3.28).

In order to further investigate possible reasons for the larger growth phenotype, stem cross-sections of each plant line were examined at various time points for changes in cell patterning, size, and shape. Sections were stained with toluidine blue and examined using light microscopy. Again, there were no apparent changes in cell morphology compared to wild-type in any of the transgenic plant lines (Figure 3.29).

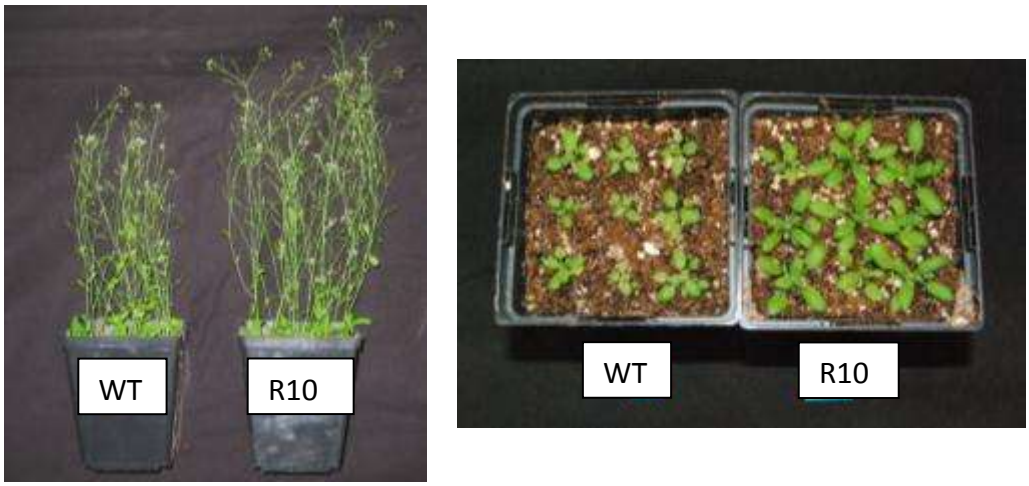


Figure 3.27. Growth of wild-type and RNAi::AtGH9C2 plants.

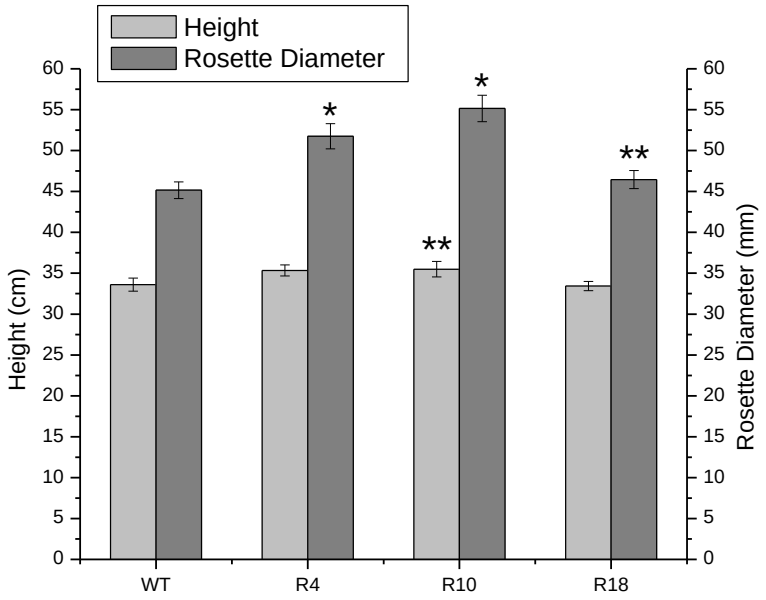


Figure 3.28. Height and rosette diameter of wild-type and RNAi::AtGH9C2 plants. (*) significant at α = 0.05; (**) significant at α = 0.10, measured using a Student's t-test (n=20).

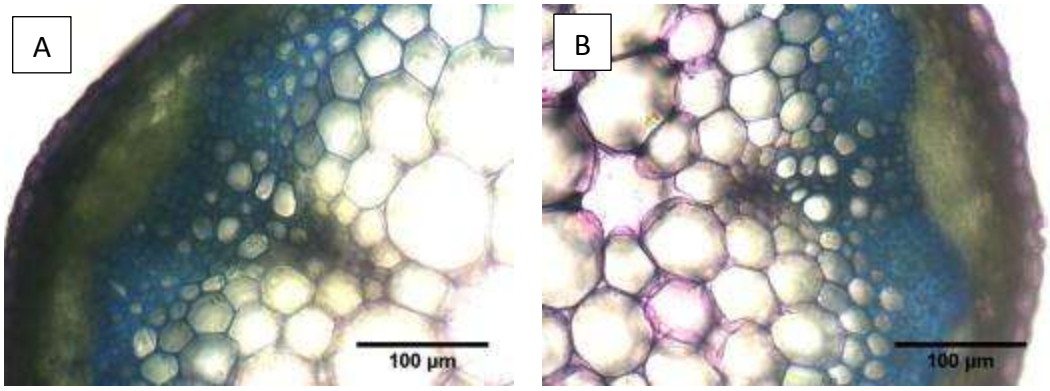


Figure 3.29. Toluidine blue stained stem cross-sections of a) wild-type, and b) RNAi::AtGH9C2 plants.

### 3.8.2 Relative expression of AtGH9C2 in RNAi::AtGH9C2 down-regulated Arabidopsis

The RNAi::AtGH9C2 construct was developed to not only down-regulate AtGH9C2, but also

At1g48930 and At4g11050, the two other Class C endoglucanases of the Arabidopsis GH9

family. However, an estimate of the expression of At1g48930 and At4g11050 in wild-type Arabidopsis cDNA by quantitative PCR, showed that the native expression of these two genes is inherently extremely low. Therefore, the primary target of the down-regulation strategy was the suppression of the main gene of interest, AtGH9C2. Quantitative PCR was used to determine the level of expression of AtGH9C2 in each plant line, which showed that lines R4, R10, and R18 showed significant down-regulation of AtGH9C2 compared to wild-type (Figure 3.30).

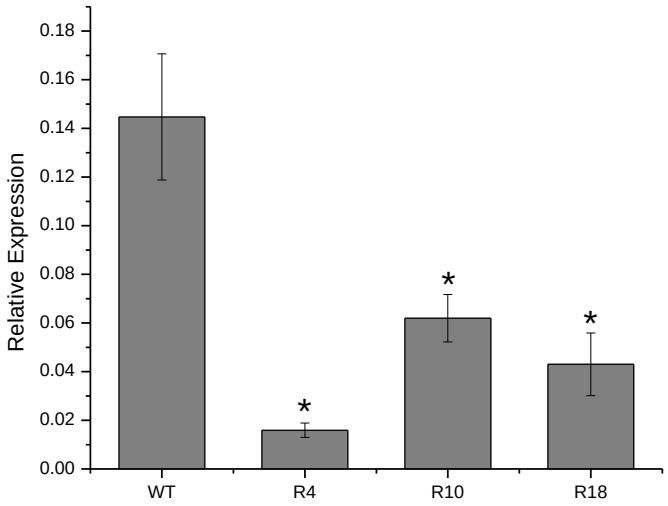


Figure 3.30. Relative expression of AtGH9C2 in wild-type and RNAi::AtGH9C2 plants. Asterisks indicate a significant difference measured using a Student's t-test at $\alpha = 0.05$ (n=3).

### 3.8.3 Cell wall crystallinity and microfibril angle

X-ray diffraction was used to measure the cell wall crystallinity and MFA of the 8-week old RNAi::AtGH9C2 dried plant stems. Crystallinity showed an average decrease of 3.1% compared to wild-type (Figure 3.31), while MFA increased in lines R4 and R10 by an average of 1.7 degrees (Figure 3.31).

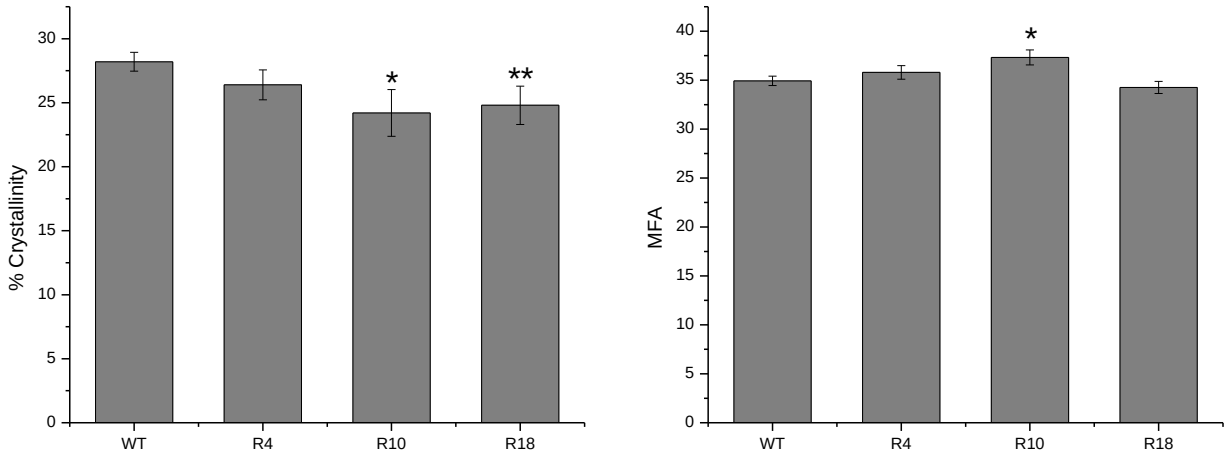


Figure 3.31. Cell wall crystallinity and MFA of wild-type and RNAi::AtGH9C2 plant stems. (*) significant at α = 0.05; (**) significant at α = 0.10, measured using a Student's t-test (n=5).

### 3.8.4 Structural carbohydrate analysis

The cell wall polysaccharides were measured by the micro-Klason method and HPLC determination. All RNAi::AtGH9C2 lines showed an increase in arabinose ranging from 3.6-17.6% (Table 3.6). Additionally, these lines showed a decrease in glucose by an average of 5.2±1.6%, and a similar decrease in xylose by 5.7±2.2% on average.

Table 3.6. Percentage of sugar per mass sample in RNAi::AtGH9C2 plant lines. Bold values indicate a significant difference measured using a Student's t-test at α = 0.10, while underlined values indicate a significant difference at α = 0.05 (n=3).

| | Arabinose | Rhamnose | Galactose | Glucose | Xylose | Mannose |
|---|---|---|---|---|---|---|
| **WT** | 0.82 (0.04) | 1.03 (0.08) | 1.64 (0.13) | 28.62 (0.43) | 11.03 (0.27) | 1.57 (0.02) |
| **R4** | **0.96 (0.03)** | 0.99 (0.06) | 1.72 (0.05) | 27.88 (1.01) | 10.75 (0.27) | 1.45 (0.14) |
| **R10** | 0.85 (0.03) | 0.97 (0.06) | 1.60 (0.02) | **26.33 (0.79)** | **9.92 (0.09)** | 1.33 (0.12) |
| **R18** | **0.99 (0.03)** | 1.07 (0.11) | 1.78 (0.11) | **27.21 (0.16)** | 10.52 (0.44) | 1.56 (0.04) |

# Chapter 4: Discussion

## 4.1 Introduction

Cell wall biosynthesis is a highly complex process that occurs as a result of the dynamic effects of various enzymes and proteins working together in a well-orchestrated manner to produce the primary cell wall, usually followed by the more rigid secondary cell wall. The process of primary cell wall development begins during cytokinesis when the cell plate is formed by the phragmoplast (Cosgrove, 1997). The phragmoplast consists of many Golgi-derived vesicles which are the source of the newly developing cell wall polysaccharides. Callose, a 1,3-β-D-glucan, is produced at the site of the growing cell plate by callose synthase, and likely plays a stabilizing role (Verma, 2001). Additionally, specific antibodies have been used to detect xyloglucan, arabinogalactan, and pectin at the cell plate. As the cell plate matures and begins to fuse with the parental plasma membrane and cell wall, callose disappears and is replaced by cellulose (Verma, 2001). The fully developed dicot primary cell wall consists mainly of the hemicellulose xyloglucan, as well as 20-30% cellulose and 30-35% pectin (Albersheim et al., 2011).

During cell expansion, there is significant turnover of cell wall components, as new components are added and the cell expands. There are two hypotheses for the incorporation of newly synthesized cell wall polysaccharides: self-assembly or enzyme-mediated assembly (Cosgrove, 1997). The self-assembly hypothesis is based on experiments which have shown that when cellulose is re-generated it replicates the allomorph of the original cellulose (Cosgrove, 1997). Similarly, when hemicelluloses are dissolved by strong alkali, they too aggregate into ordered networks (Cosgrove, 1997). This theory is attractive in its simplicity, however, it has also been

shown that the xyloglucan complexes formed with cellulose *in vitro* are less stable than those in natural plant cell walls, suggesting that this process may normally be assisted by various proteins (Cosgrove, 1997).

As more research accumulates on carbohydrate active enzymes, it is becoming increasingly apparent that enzyme-mediated assembly likely plays a larger role in cell wall development. Some of the enzymes proposed to play a role in these processes have been mentioned previously, such as XTHs which are capable of cleaving xyloglucan chains as well as linking them together, and perhaps facilitate the incorporation of newly synthesized xyloglucan chains into the cell wall network (Eklof & Brumer, 2010). Expansins are proteins that are thought to interrupt the association of xyloglucan and cellulose microfibrils permitting them to slide apart during cell expansion (McQueen-Mason, 1995), while pectin methylesterases may enhance the ability of pectin to form calcium bridges, which in turn solidifies the pectin gel network (Caffall & Mohnen, 2009). Of particular interest to this study, is the role that β-1,4-D-endoglucanases may play in cell wall modification. These enzymes are predicted to cleave β-1,4-glucan bonds and are therefore projected to act on cellulose and/or xyloglucans, and have been implicated in cell wall modification (Libertini et al., 2004). In support of this hypothesis, a previous study showed that the application of endoglucanases to isolated heat-inactivated walls did not yield much expansion, however, when expansins were applied subsequently extension was greater than application without prior treatment by endoglucanases, thereby indirectly implicating endoglucanases in cell expansion (Cosgrove & Durachko, 1994).

Secondary cell wall development is thought to occur once primary cell wall expansion ceases, however, the molecular underpinning of this transition remains unclear. There have been several studies that identify which genes are up- and down-regulated during the switch from primary cell wall production to secondary cell wall development (Brown et al., 2005; Dharmawardhana et al., 2010; Zhong et al., 2008). NAC domain transcription factors, such as SND1, have proven to be essential for secondary cell wall development as they regulate the expression of an entire group of genes required for secondary cell wall synthesis (Zhong et al., 2008). Furthermore, different cell types appear to have different "master" transcriptional switches, for example, VND6 and VND7 in vessel elements ((Kubo et al., 2005)), and NST1 and NST2 in the endothecium of anthers (Zhong et al., 2008). Overexpression of any one of these genes results in ectopic secondary cell wall deposition, and down-regulation results in impaired secondary cell wall thickening. Although the transcriptional regulation of secondary cell wall development has been fairly well-studied, the physical process and timing of the remodelling of the cell wall requires further investigation. Nevertheless, the end result of secondary cell wall development is a wall that is made up of approximately 37-57% cellulose, 17-30% lignin, 20-37% hemicellulose (mostly xylans), and less than 10% pectin (Albersheim et al., 2011). The final cell wall is a mechanically strong and enzymatically recalcitrant structure which enables plants to grow to great heights and survive diverse biotic and abiotic factors.

## 4.2 Role of Class B endoglucanases AtGH9B5 and PtGH9B5

### 4.2.1 Expression patterns of AtGH9B5 and PtGH9B5

An analysis of 20 poplar transcriptomes identified the *P. trichocarpa* endoglucanase PtGH9B5 as having high xylem transcript abundance. The endoglucanase orthologous to KORRIGAN showed

the highest expression of the entire GH9 family, followed by PtGH9B5, then PtGH9C2. The availability of leaf transcriptome data for the same study (n=3) made it possible to calculate the xylem:leaf ratio of PtGH9B5 expression, which was found to be 2.5. This suggests that this endoglucanase is highly expressed during secondary cell wall development in poplar, and does not play as large a role in the development of other organs, such as leaves. Arabidopsis expression data from the University of Toronto BioBar website provided additional information on the expression pattern of the Arabidopsis ortholog AtGH9B5 (Winter et al., 2007). Consistent with the observed expression data derived from the poplar transcriptome data, the expression of this gene is mainly observed in the second internode of the stem (Figure 4.1), where secondary cell wall development is expected to occur (Winter et al., 2007).

The University of Toronto BioBar website also provides information on genes that are co-expressed with a gene of interest (Toufighi et al., 2005). Analysis of AtGH9B5 suggests that it is co-regulated with the secondary cell wall specific gene AtCSLA9 (At5g03760) which is a cellulose-synthase-like gene predicted to be involved in mannose synthesis (Liepman & Cavalier, 2012). Additionally, AtGH9B5 is co-expressed with the Class C endoglucanase At4g11050 (AtGH9C3) which is expressed mainly in the stem and foliar organs. As AtGH9B5 can also be seen to have high expression in mature pollen, it is not surprising that it is also co-expressed with genes involved in pollen development such as members of the pectate lyase family and certain arabinogalactan protein (AGP) genes.

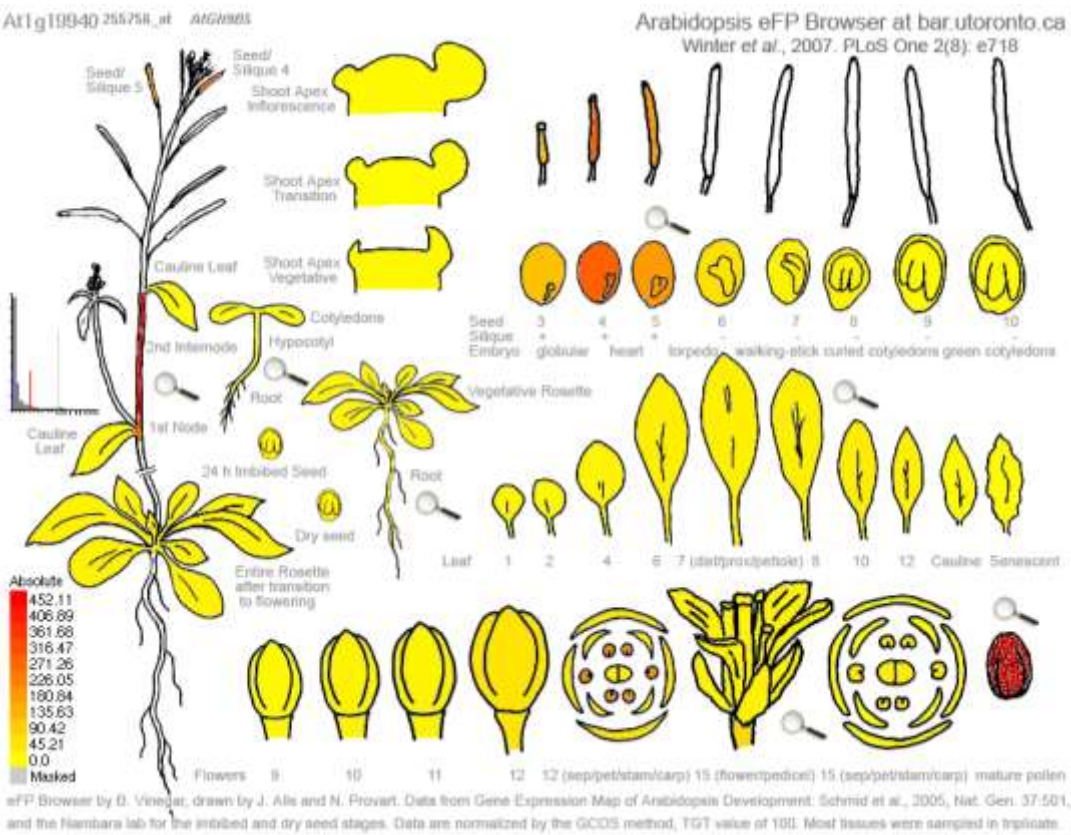


Figure 4.1. Expression pattern of AtGH9B5 in Arabidopsis (Winter et al., 2007).

### 4.2.2 Proposed function of AtGH9B5/PtGH9B5

AtGH9B5 is a Class B endoglucanase consisting of a catalytic domain and a signal peptide for secretion to the cell wall. Unlike other members of its class, this endoglucanase has been predicted to have a GPI anchor (Schwacke et al., 2003). GPI anchors are synthesized by enzymes associated with the endoplasmic reticulum, which is also the site of transfer of the target protein to the anchor (Gillmor et al., 2005). The final destination of GPI-anchored proteins is the extracellular face of the plasma membrane. There are several predicted roles for the GPI anchor, including acting as a link between the plasma membrane and the developing cell wall, activation of the protein by cleavage of the GPI anchor, targeting of the protein proximal to its primary function beneath the cell wall, or co-targeting of proteins that can function more

efficiently if close to one another (Borner et al., 2002). A study on the cells of the seedling-lethal Arabidopsis mutant *pnt1*, which is deficient in a mannosyltransferase required for GPI anchor synthesis, resulted in cell walls that had reduced crystalline cellulose and increased levels of pectin, suggesting that GPI anchors are indeed required for cell wall synthesis, as well as for plant development (Gillmor et al., 2005).

While the function of the AtGH9B5/PtGH9B5 GPI anchor has not yet been directly examined, there have been studies that confirm the association of this endoglucanase with the plasma membrane. A recent analysis of plasma membrane associated proteins in developing xylem and phloem of poplar trees resulted in the purification of the PtGH9B5 peptide, as well as the poplar ortholog of KORRIGAN (Song et al., 2011). Both endoglucanases were present in plasma membrane fractions of phloem and xylem preparations. A similar study by Nilsson et al. (2010) also demonstrated that PtGH9B5 (as well as KORRIGAN) is associated with the plasma membrane, however, the peptide was found only in the plasma membrane fraction of fully-grown leaf tissue (Nilsson et al., 2010). It is possible that the difference in localization of PtGH9B5 in these two studies is a function of sample collection, as the samples in the Nilsson et al. (2010) study came from bulk phloem and xylem scrapings near the base of the tree, while Song et al. (2011) specifically collected only the differentiating xylem and phloem cells from the upper part of the stem.

The possible function of AtGH9B5 in the plant cell wall has only briefly been touched upon. The change in transcript level of AtGH9B5 was measured in Arabidopsis stem segments after a weight had been applied to the plant stem (Koizumi et al., 2009). The expression of the gene

was up-regulated in the region just below the weight, suggesting that this gene is involved in maintaining supportive tissue. Furthermore, a promoter::GUS experiment showed that AtGH9B5 was primarily expressed in the interfascicular xylem region of stem cross-sections (Koizumi et al., 2009). The GUS expression was also noted in the anthers and leaf vessels, further confirming that this endoglucanase likely plays a role in secondary cell wall development. This finding is in agreement with the poplar transcriptome and Arabidopsis expression data previously discussed, as well as with the observation that expression of PtGH9B5 under control of the secondary cell wall specific CesA8 promoter resulted in a change in growth while the constitutive 35S promoter did not.

Furthermore, structural sugar analysis may also point to a role for AtGH9B5 providing a supportive role in cell walls. In the t-DNA mutant, glucose and xylose were decreased, while in the AtCesA8pr overexpression plant lines, glucose and xylose were increased. Secondary cell wall development is marked by an increase in cellulose and xylans, which provide mechanical strength (Persson et al., 2007). Synthesis of new cellulose microfibrils has been suggested to be followed by the release of xylans into the secondary cell wall, coating the cellulose microfibrils (Awano et al., 2002). Additionally, once the cellulose microfibrils are coated, it is thought that xylan continues to be deposited and penetrates the cell wall to form globular deposits on the cellulose microfibrils, immediately prior to lignification (Awano et al., 2002). Since there is evidence to suggest that this protein is associated with the plasma membrane and is expressed during secondary cell wall development, it is possible that this endoglucanase could play a role in facilitating the integration of xylans into the secondary cell wall. If newly deposited xylans near the plasma membrane cannot integrate into the cell wall, perhaps a feedback mechanism

exists which prevents more xylans from being released into the cell wall. Furthermore, if there are excess xylans at the plasma membrane, it is possible that this may also affect the amount of cellulose entering the cell wall. This theory could explain why the down-regulation of AtGH9B5 results in less xylose and glucose, and defines a role for this enzyme in maintaining secondary cell wall mechanical strength. Therefore, the smaller growth phenotype of the AtCesA8pr overexpression plant lines may be the result of accelerated secondary cell wall development bringing primary growth to a more abrupt stop. Interestingly, crystallinity appears to show an increasing trend in both the t-DNA mutant and the AtCesA8pr overexpression lines. If AtGH9B5/PtGH9B5 also plays a role in regulating cellulose crystallinity, it is possible that a decrease in the xylose and glucose content in the t-DNA mutants is off-set by an increase in crystallinity, perhaps by another endoglucanase acting either independently or in a semi-redundant manner.

## 4.3 Role of Class C endoglucanases AtGH9C2 and PtGH9C2

### 4.3.1 Expression patterns of AtGH9C2 and PtGH9C2

The analysis of poplar transcriptome data also identified the endoglucanase PtGH9C2 as being the third highest annotated endoglucanase expressed during active xylem growth compared to the remaining GH9 family. Upon further examination of the transcriptome data, it was found that this endoglucanase is also highly expressed in the leaf, with a xylem:leaf ratio of 0.69. This suggests that this endoglucanase is not only expressed during secondary cell wall development, but during cell wall development in general. The expression pattern of the Arabidopsis ortholog AtGH9B5 was examined using the University of Toronto BioBar website (Winter et al., 2007). In agreement with the poplar transcriptome data, expression of AtGH9C2 is observed in many

different tissues, primarily in the first node and second internode of the stem, the hypocotyl, and rosette leaves (Figure 4.2). Co-expression analysis of AtGH9C2 shows that it is expressed along with several genes that are known to play a role in plant stem development, such as the pectin lyase gene At1g04680, as well as cellulose synthase-like C5 (At4g31590) which is putatively involved in the synthesis of the β-1,4-glucan backbone of xyloglucan (Cocuron et al., 2007). Therefore, the expression of this gene in a variety of tissues supports the idea that this endoglucanase is involved in not only secondary but general cell wall development.

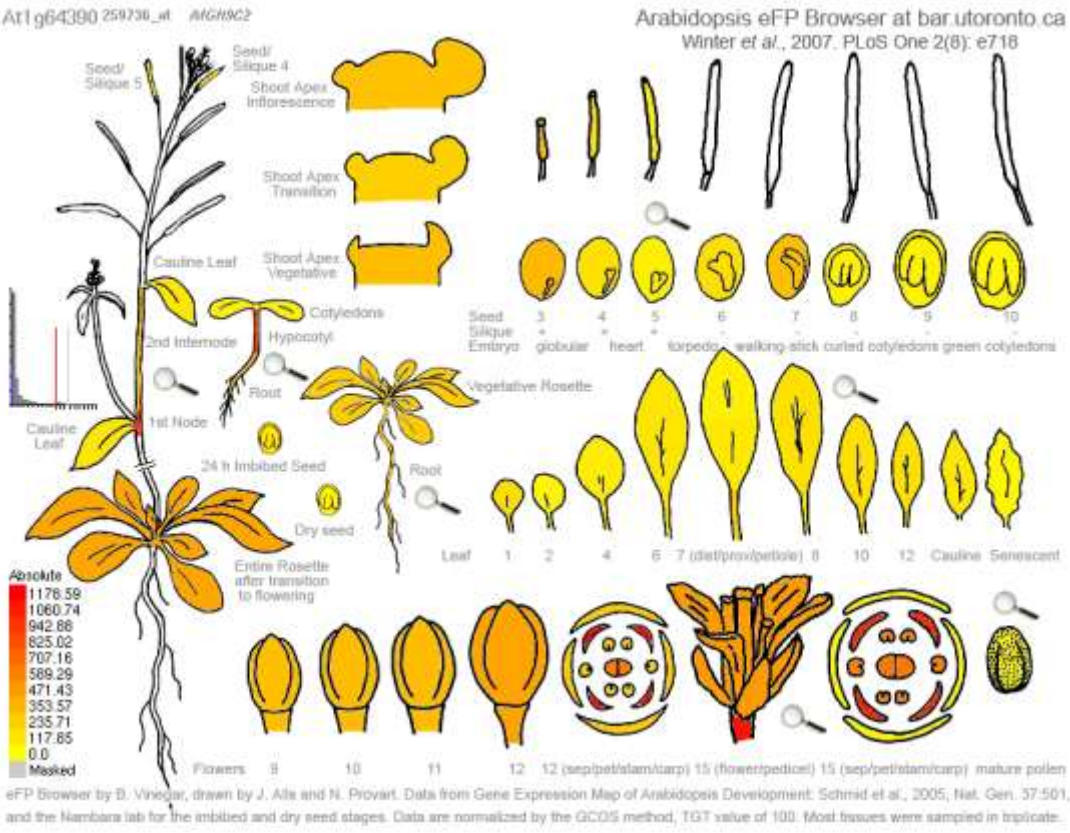


Figure 4.2. Expression pattern of AtGH9C2 in Arabidopsis (Winter et al., 2007).

### 4.3.2 Potential cell wall substrate of AtGH9C2 and PtGH9C2

AtGH9C2 is a unique endoglucanase of glycosyl hydrolase family 9, as it is one of only three which contain a novel carbohydrate-binding module, CBM49 (Urbanowicz et al., 2007). Carbohydrate-binding modules (CBMs) are typically present in microbial endoglucanases, allowing them to bind to crystalline cellulose, and have long been thought to be absent in plant endoglucanases until recently (Libertini et al., 2004). It is largely for this reason that plant endoglucanases have been predicted to only have activity on non-crystalline regions of cellulose, as well as xyloglucan.

CBMs are non-catalytic domains which can be found attached to glycoside hydrolases by a linker region, and are predicted to play three potential roles: bringing the catalytic domain close to its target substrate, targeting the catalytic domain to the correct substrate, and/or disrupting the substrate for easier enzymatic access (Boraston et al., 2004). Type A CBMs generally bind to the surface of crystalline polysaccharides, while the attached catalytic domain is active on other polysaccharides. In contrast, Type B CBMs bind directly to their target polysaccharide, and the less common Type C CBMs bind to mono, di, or tri-saccharides (Boraston et al., 2004).

Urbanowicz et al. (2007) first characterized CBM49 in a tomato (*Solanum lycopersicum*) glycosyl hydrolase family 9 endoglucanase (SlCel9C1), and found that it was most similar to the microbial family CBM2 and, more specifically, shared the same conserved tryptophan residues experimentally confirmed to be critical for binding of the *Cellumonas fimi* CBM2a to cellulose. This microbial Type A CBM has been suggested to play a role in the disruption of the crystalline structure of cellulose, enhancing the degradative ability of the catalytic domain (Boraston et al., 2004). However, the overall amino acid similarity of the SlCel9C1 CBM to CBM2a is too low to

make any inferences regarding its possible function in the plant cell wall (Urbanowicz et al., 2007). Further characterization of CBM49 by Urbanowicz et al. (2007) suggested that this CBM can in fact bind to crystalline cellulose almost as effectively as CBM2a at high substrate concentrations. Yoshida et al. (2006a) studied the rice ortholog (OsCel9A) and found that they could not isolate the full-length protein containing the intact CBM. Antibodies specific to the truncated and full-length protein were used to detect which form is present in the buffer-soluble, microsomal membrane, and cell wall fraction of root tissue in rice. The full-length protein existed predominately in the microsomal membrane fraction, while the truncated protein was the predominant form in the soluble fraction, and neither form was associated with the cell wall bound fraction. Additionally, only the soluble fraction displayed enzymatic activity, leading the authors to suggest that the full-length protein is inactive until it reaches its target in the cell wall, at which point the CBM is cleaved via proteolysis, activating the catalytic domain in close proximity to its target. Alignment of AtGH9C2 and PtGH9C2 with the tomato and rice CBMs, confirmed the presence of the conserved tryptophan residues of the *C. fimi* CBM2a, suggesting the plant CBMs may play a similar role. However, CBM studies have been largely based on microbes, therefore it is difficult to predict whether or not plant CBMs have a similar function.

In addition to characterizing CBM49, Urbanowicz et al. (2007) and Yoshida et al. (2006b) also conducted substrate binding/activity assays with the catalytic domains of their respective recombinant proteins. Urbanowicz et al. (2007) found that the catalytic domain had the highest activity on a mixed-linkage glucan (MLG), followed by arabinoxylan, medium and low viscosity carboxymethyl cellulose, and only slight activity on xyloglucan. Yoshida et al. (2006b) achieved

similar results, showing that the catalytic domain had highest activity on carboxymethyl cellulose, followed by MLG, arabinoxylan, and only trace activity on xyloglucan. Xyloglucan has long been suggested to be a potential target of plant endoglucanases as this hemicellulose has a β-1,4-glucan backbone, similar to cellulose. Therefore, it is of great interest that these studies suggest that these endoglucanases are not active on xyloglucan.

In the current study, the cell wall carbohydrate compositional analysis shows that the amount of xylose decreased in both the AtCesA8pr::PtGH9C2 and RNAi::AtGH9C2 lines. This suggests that there may be some kind of compensatory action occurring in the RNAi lines in order to mitigate the lack of AtGH9C2. Because the glycosyl hydrolase family is fairly large, it is possible that some of the endoglucanases have redundant functions. AtGH9B7 is a Class B endoglucanase that is also co-expressed with AtGH9C2. This endoglucanase has not been studied to date, but the University of Toronto BioBar website (Winter et al., 2007) suggests that it is expressed in the same tissues as AtGH9C2, particularly in the stem. Because the changes in structural carbohydrates are similar in the AtCesA8pr and RNAi lines, but the crystallinity and growth phenotype of these plant lines differs, it is possible that AtGH9B7 is partially redundant with AtGH9C2. In two of the AtCesA8pr lines, glucose and xylose both decrease, which could point to an effect on xyloglucan, however, given previous research (Urbanowicz et al., 2007; Yoshida & Komae, 2006b) and the fact that the other two lines show no change in glucose, it may be more likely that the changes have occurred on the level of xylans. The only clear opposing trend in structural sugars of these plant lines is the decrease in arabinose in the AtCesA8pr overexpression lines and subsequent increase in the RNAi down-regulation lines, however, the role of this enzyme in moderating the amount of arabinose is unclear. Though the

rice and tomato studies suggest arabinoxylan as a potential substrate, this hemicellulose only makes up ~5% of the dicot primary cell wall (Albersheim et al., 2011). Additionally, MLG is not a component of dicot cell walls. Therefore, although it is unclear how the overall structural sugar content of the transgenic plant lines has changed, it is possible that this endoglucanase may play a role in the remodelling of the cell wall, and therefore may play a role in regulating cell expansion as the changes in growth form of the transgenic plants suggests.

### 4.3.3 Proposed function of AtGH9C2 and PtGH9C2

The most striking phenotypic change in the AtCesA8pr overexpression and RNAi plant lines was the effect on plant height and rosette diameter. Overexpressing PtGH9C2 led to a decrease in height and rosette diameter, while down-regulation of AtGH9C2 led to an increase in height and rosette diameter. This corresponded with an increase in cell wall crystallinity in the overexpressing lines and a decrease in the down-regulated lines. The effect of cellulose crystallinity on cell expansion has mostly been studied in primary cell walls, where it was found that rapidly growing dark-grown hypocotyls had a lower degree of crystallinity than slower growing light-grown hypocotyls (Fujita et al., 2011; Harris & DeBolt, 2008). Evidence suggests that xyloglucan is more capable of binding with amorphous regions of cellulose (Lai-Kee-Him et al., 2002), therefore low crystallinity may result in more xyloglucan cross-linking, enabling anisotropic cell expansion (Fujita et al., 2011). Additionally, expansins have been suggested to have a higher affinity for non-crystalline cellulose that is associated with other matrix polysaccharides (McQueen-Mason, 1995), and therefore, this may also contribute to the increased growth rate associated with the observed decrease in cell wall crystallinity.

The expression of PtGH9C2 in xylem suggests its involvement in secondary cell wall development; however, it is also expressed highly in leaves, suggesting that this gene may also play a more general role in cell wall development. Given the change in cell wall crystallinity in the overexpressing and down-regulated plant lines, it is possible that this endoglucanase plays a role in regulating the degree of crystallinity in the newly forming secondary cell wall. Perhaps by CBM targeting to crystalline cellulose prior to proteolytic cleavage, this enzyme can regulate cross-linking with matrix polysaccharides, maintaining the crystallinity of the newly synthesized secondary cell wall cellulose microfibrils, and limiting cell expansion. If this enzyme is in fact active on xylans, then the decrease in xylose in the AtCesA8pr overexpression lines suggests that this enzyme reduces the amount of xylans available for secondary cell wall cellulose cross-linking, thereby maintaining cell wall crystallinity. In the RNAi lines, it is possible that partial redundancy by another endoglucanase, such as AtGH9B7, is able to mitigate the change in xylans, and that the lack of a CBM associated with this enzyme leaves it unable to regulate the degree of crystallinity, thereby resulting in the mutant phenotype.

Although secondary cell wall development is generally thought to begin once the primary cell wall has ceased expansion, the exact mechanism facilitating/regulating the transition is unknown and it remains a possibility that these two developmental stages occur synchronously to some extent. As described by Fujita et al. (2011), the degree of crystallinity may regulate the rate of expansion of the primary cell wall through fewer cross-links with hemicelluloses (Lai-Kee-Him et al., 2002) and decreased action of expansins (McQueen-Mason, 1995). Therefore, if overexpression of PtGH9C2 by the AtCesA8pr results in a greater degree of crystallinity during early secondary cell wall development, perhaps this enzyme plays a role in cessation of primary

growth, thereby resulting in the smaller plant growth phenotype observed in these transgenic plant lines, and larger growth phenotype of the reduced crystallinity RNAi plants.

# Chapter 5: Conclusions

## 5.1 AtGH9B5 and PtGH9B5 thesis summary

The endoglucanases AtGH9B5 and PtGH9B5 are Class B endoglucanases, both predicted to have a GPI anchor (Schwacke et al., 2003). Expression analysis of poplar transcriptome data showed high expression in xylem, pointing to a role for PtGH9B5 in secondary cell wall development and analysis of Arabidopsis expression data confirmed the expression of AtGH9B5 in stem tissue (Winter et al., 2007). Furthermore, two studies on plasma membrane-associated proteins in poplar xylem and phloem, confirm the association of PtGH9B5 with the plasma membrane (Nilsson et al., 2010; Song et al., 2011), as well as its expression in xylem (Song et al., 2011).

Structural carbohydrate analysis of the *atgh9b5* t-DNA insertion mutant and AtCesA8pr::PtGH9B5 transgenic plant lines showed opposing effects on the percentage of glucose and xylose in stem tissue. In a study by Koizumi et al. (2009), a promoter::GUS experiment using the native AtGH9B5 promoter showed that this promoter is active in the interfascicular region of Arabidopsis stem cross-sections, suggesting a role for this endoglucanase in supportive tissue. Given that an increase in cellulose and xylans during secondary cell wall development is thought to provide mechanical strength to the cell wall, it is possible that AtGH9B5 and PtGH9B5 play a role in the regulation or integration of these cell wall polysaccharides. Because glucose and xylose decrease in the t-DNA insertion mutant and increase in the AtCesA8pr::PtGH9B5 transgenic plant lines, it is possible that this enzyme enables the incorporation of cellulose and/or xylans into the developing secondary cell wall, increasing its mechanical strength. Additionally, an increase in crystallinity was observed in the

AtCesA8pr plants, further supporting the role of this enzyme in stabilizing the secondary cell wall.

### 5.1.1 Future research

The substrate of plant endoglucanases has long been thought to be either amorphous regions of cellulose or xyloglucan. However, there have been few studies that have actually tested the binding activity of the various endoglucanases. From this study, it appears that AtGH9B5 and PtGH9B5 affect the incorporation of xylans and/or cellulose into the developing secondary cell wall, however, more evidence is required to prove this theory. Therefore, it would be of great interest to isolate a full-length, mature protein which can be used to test the substrate binding specificity of this enzyme.

Because of the promoter activity observed in the interfascicular fibres (Song et al., 2011) and the observed effects on glucose and xylose in the genetically modified plant lines, it has been suggested that this enzyme plays a role in providing mechanical strength to the secondary cell wall. It would be beneficial to test this theory by examining the micromechanics of these plants using a three-point bending test. Furthermore, given the change in crystallinity of the transgenic plant lines, it would be of interest to examine the degree of polymerization of the cellulose microfibrils, as this has also been predicted to affect the strength of the cell wall (Wasteneys & Fujita, 2006).

## 5.2 AtGH9C2 and PtGH9C2 thesis summary

The Class C endoglucanase PtGH9C2 was determined to be highly expressed in xylem and leaves based on poplar transcriptome data, and expression of AtGH9C2 in Arabidopsis shows a similar pattern. This suggests that this enzyme is not just involved in secondary cell wall

development, but cell wall development in general. The presence of a carbohydrate binding module is a unique component of these endoglucanases which has not been previously studied in Arabidopsis or poplar. Studies in tomato and rice orthologs suggest that this CBM is capable of binding to crystalline cellulose (Urbanowicz et al., 2007; Yoshida et al., 2006a), but may be post-translationally cleaved after it enters the extracellular space (Yoshida et al., 2006a). Although the genetically modified plants in this study did not show clear changes in structural carbohydrates apart from the level of xylose, there was a decreasing trend in crystallinity in the RNAi::AtGH9C2 lines and an increasing trend in crystallinity in the AtCesA8pr::AtGH9C2 lines, suggesting that this endoglucanase may play a role in regulating the degree of crystallinity in the cell wall. Additionally, these plants were different in height and rosette diameter. If the CBM does in fact bind to cellulose before proteolysis, this enzyme may function by being targeted to the newly synthesized cellulose chain, thereby regulating the association between cellulose and other cell wall polysaccharides, such as xylans, maintaining the degree of crystallinity. By doing so, it is possible that this enzyme may be involved in primary growth cessation, contributing to the contrasting growth phenotypes identified in the AtCesA8pr and RNAi plant lines.

### 5.2.1 Future research

The change in crystallinity observed in the RNAi::AtGH9C2 and AtCesA8pr::PtGH9C2 plant lines suggests that this enzyme is involved in regulating the degree of crystallinity in the cell wall, however, the mechanism that is involved in this is unknown. In order to better assess the degree of crystallinity, it would be of interest to measure Updegraff cellulose (Updegraff, 1969). This measurement would also help to elucidate the changes occurring in the structural

carbohydrates, as it is currently unknown whether changes in glucose can be ascribed to a change in cellulose or a change in the glucose content associated with the hemicelluloses. Additionally, because endoglucanases are predicted to be non-processive and therefore potentially able to cleave the cellulose chain at various intervals, it is possible that they may have an effect on the degree of polymerization of cellulose. This may weaken the cellulose chain, and may also affect its degree of crystallinity. If cellulose is in fact the substrate of the AtGH9C2 and PtGH9C2 CBM, these enzymes may regulate crystallinity by controlling the proportion of amorphous regions in the crystalline cellulose chain, limiting the interaction of cellulose with other cell wall polysaccharides, such as xylans.

## 5.3 Research significance

The Arabidopsis endoglucanase family consists of 25 members, many of which have not yet been studied. To date, the most extensively researched endoglucanase is KORRIGAN (At5g49720), which has been shown to play a significant role in cellulose biosynthesis, though its exact function in this respect remains unclear. Of the 25 genes in this family, the poplar ortholog of KORRIGAN was most highly expressed in xylem from poplar transcriptome data, but two other endoglucanases also showed high expression: PtGH9B5 and PtGH9C2. These endoglucanases represent the next most highly up-regulated endoglucanase genes in xylem, as most others showed very little expression in this tissue. Although the role of these endoglucanases in cell wall development is still uncertain, some advances in fundamental knowledge have been made. PtGH9B5 and its Arabidopsis ortholog AtGH9B5 have been identified as plasma membrane proteins, and glucose and/or xylose have been suggested as potential substrates for these enzymes. Additionally, overexpression of PtGH9B5 using a

promoter specific to secondary cell wall development (AtCesA8pr), led to a decrease in plant height and rosette diameter, suggesting this gene can affect cell expansion. Overexpression of PtGH9C2 and down-regulation of AtGH9C2 led to changes in the degree of cell wall crystallinity, suggesting that these enzymes may play a role in regulating this important characteristic. Furthermore, the degree of crystallinity inversely correlated with a change in plant height and rosette diameter, suggesting that this protein may be active during the transition from primary to secondary growth, and may play a role in limiting primary cell expansion. Overall, progress has been made in understanding the role of these two endoglucanases, however, the results have only just begun to lay the foundation for more in depth research.

# References


Albersheim, P., Darvill, A., Roberts, K., Sederoff, R., & Staehelin, A. (2011). *Plant cell walls*. New York: Garland Science, Taylor & Francis Group, LLC.

Awano, T., Takabe, K., & Fujita, M. (2002). Xylan deposition on secondary wall of *Fagus crenata* fiber. *Protoplasma, 219*(1), 106-115.

Barnett, J. R., & Bonham, V. A. (2004). Cellulose microfibril angle in the cell wall of wood fibres. *Biological Reviews, 79*(2), 461-472.

Boraston, A., Bolam, D., Gilbert, H., & Davies, G. (2004). Carbohydrate-binding modules: Fine-tuning polysaccharide recognition. *Biochemical Journal, 382*(Pt 3), 769-781.

Borner, G. H. H., Sherrier, D. J., Stevens, T. J., Arkin, I. T., & Dupree, P. (2002). Prediction of glycosylphosphatidylinositol-anchored proteins in arabidopsis. A genomic analysis. *Plant Physiology, 129*(2), 486-499.

Brown, D. M., Zeef, L. A. H., Ellis, J., Goodacre, R., & Turner, S. R. (2005). Identification of novel genes in arabidopsis involved in secondary cell wall formation using expression profiling and reverse genetics. *The Plant Cell Online, 17*(8), 2281-2295.

Caffall, K. H., & Mohnen, D. (2009). The structure, function, and biosynthesis of plant cell wall pectic polysaccharides. *Carbohydrate Research, 344*(14), 1879-1900.

Cannon, M. C., Terneus, K., Hall, Q., Tan, L., Wang, Y., Wegenhart, B. L., et al. (2008). Self-assembly of the plant cell wall requires an extensin scaffold. *Proceedings of the National Academy of Sciences, 105*(6), 2226-2231.

Cantarel, B. L., Coutinho, P. M., Rancurel, C., Bernard, T., Lombard, V. & Henrissat, B. (2009). *The carbohydrate-active EnZymes database (CAZy): An expert resource for glycogenomics.* Retrieved July, 2010, from http://www.cazy.org/

Cocuron, J., Lerouxel, O., Drakakaki, G., Alonso, A. P., Liepman, A. H., Keegstra, K., et al. (2007). A gene from the cellulose synthase-like C family encodes a beta-1,4 glucan synthase. *Proceedings of the National Academy of Sciences, 104*(20), 8550-8555.

Coleman, H. D., Yan, J., & Mansfield, S. D. (2009). Sucrose synthase affects carbon partitioning to increase cellulose production and altered cell wall ultrastructure. *Proceedings of the National Academy of Sciences,*

Cosgrove, D. J. (2005). Growth of the plant cell wall. *Nature, 6*, 850-861.

Cosgrove, D. J., & Durachko, D. M. (1994). Autolysis and extension of isolated walls from growing cucumber hypocotyls. *Journal of Experimental Botany,* (45), 1711.

Cosgrove, D. J. (1997). Assembly and enlargement of the primary cell wall in plants. *Annual Review of Cell and Developmental Biology, 13*(1), 171-201.

Curtis, M. D., & Grossniklaus, U. (2003). A gateway cloning vector set for high-throughput functional analysis of genes in planta. *Plant Physiology, 133*(2), 462-469.

Desprez, T., Juraniec, M., Crowell, E. F., Jouy, H., Pochylova, Z., Parcy, F., et al. (2007). Organization of cellulose synthase complexes involved in primary cell wall synthesis in arabidopsis thaliana. *Proceedings of the National Academy of Sciences, 104*(39), 15572-15577.

Dharmawardhana, P., Brunner, A., & Strauss, S. (2010). Genome-wide transcriptome analysis of the transition from primary to secondary stem development in populus trichocarpa. *BMC Genomics, 11*(1), 150.

Edwards, K., Johnstone, C., & Thompson, C. (1991). A simple and rapid method for the preparation of plant genomic DNA for PCR analysis. *Nucleic Acids Research, 19*(6), 1349-1349.

Eklof, J. M., & Brumer, H. (2010). The XTH gene family: An update on enzyme structure, function, and phylogeny in xyloglucan remodeling. *Plant Physiology, 153*(2), 456-466.

Fujita, M., Himmelspach, R., Hocart, C. H., Williamson, R. E., Mansfield, S. D., & Wasteneys, G. O. (2011). Cortical microtubules optimize cell-wall crystallinity to drive unidirectional growth in arabidopsis. *The Plant Journal, 66*(6), 915-928.

Geraldes, A., Pang, J., Thiessen, N., Cezard, T., Moore, R., Zhao, Y., et al. (2011). SNP discovery in black cottonwood (populus trichocarpa) by population transcriptome resequencing. *Molecular Ecology Resources, 11*, 81-92.

Gillmor, C. S., Lukowitz, W., Brininstool, G., Sedbrook, J. C., Hamann, T., Poindexter, P., et al. (2005). Glycosylphosphatidylinositol-anchored proteins are required for cell wall synthesis and morphogenesis in arabidopsis. *The Plant Cell Online, 17*(4), 1128-1140.

Goda, H., Sawa, S., Asami, T., Fujioka, S., Shimada, Y., & Yoshida, S. (2004). Comprehensive comparison of auxin-regulated and brassinosteroid-regulated genes in arabidopsis. *Plant Physiology, 134*(4), 1555-1573.

Goulao, L. F., Vieira-Silva, S., & Jackson, P. A. (2011). Association of hemicellulose- and pectin-modifying gene expression with eucalyptus globulus secondary growth. *Plant Physiology and Biochemistry, 49*(8), 873-881.

Gutierrez, L., Mauriat, M., Guenin, S., Pelloux, J., Lefebvre, J., Louvet, R., et al. (2008). The lack of a systematic validation of reference genes: A serious pitfall undervalued in reverse transcription-polymerase chain reaction (RT-PCR) analysis in plants. *Plant Biotechnology Journal, 6*(6), 609-618.

Hamann, T., Osborne, E., Youngs, H. L., Misson, J., Nussaume, L., & Somerville, C. (2004). Global expression analysis of *CESA* and *CSL* genes in arabidopsis. *Cellulose, 11*(3), 279-286.

Harris, D., & DeBolt, S. (2008). Relative crystallinity of plant biomass: Studies on assembly, adaptation and acclimation. *PLoS ONE, 3*(8), e2897.

Helliwell, C., & Waterhouse, P. (2003). Constructs and methods for high-throughput gene silencing in plants. *Methods, 30*(4), 289-295.

Karimi, M., De Meyer, B., & Hilson, P. (2005). Modular cloning in plant cells. *Trends in Plant Science, 10*(3), 103-105.

Koizumi, K., Yokoyama, R., & Nishitani, K. (2009). Mechanical load induces upregulation of transcripts for a set of genes implicated in secondary wall formation in the supporting tissue of arabidopsis thaliana. *Journal of Plant Research, 122*(6), 651-659.

Kubo, M., Udagawa, M., Nishikubo, N., Horiguchi, G., Yamaguchi, M., Ito, J., et al. (2005). Transcription switches for protoxylem and metaxylem vessel formation. *Genes & Development, 19*(16), 1855-1860.

Lai-Kee-Him, J., Chanzy, H., Muller, M., Putaux, J., Imai, T., & Bulone, V. (2002). In vitro versus in VivoCellulose microfibrils from plant primary wall synthases: Structural differences. *Journal of Biological Chemistry, 277*(40), 36931-36939.

Lane, D. R., Wiedemeier, A., Peng, L., Hofte, H., Vernhettes, S., Desprez, T., et al. (2001). Temperature-sensitive alleles of RSW2 link the KORRIGAN endo-1,4-beta-glucanase to cellulose synthesis and cytokinesis in arabidopsis. *Plant Physiology, 126*(1), 278-288.

Libertini, E., Li, Y., & McQueen-Mason, S. (2004). Phylogenetic analysis of the plant endo-beta-1,4-glucanase gene family. *Journal of Molecular Evolution, 58*(5), 506-515.

Liepman, A. H., & Cavalier, D. M. (2012). The CSLA and CSLC families: Recent advances and future perspectives. *Frontiers in Plant Science, 3*

Lopez-Casado, G., Urbanowicz, B. R., Damasceno, C. M. B., & Rose, J. K. C. (2008). Plant glycosyl hydrolases and biofuels: A natural marriage. *Current Opinion in Plant Biology, 11*, 329-337.

Maloney, V. J., & Mansfield, S. D. (2010). Characterization and varied expression of a membrane-bound endo-b-1,4-glucanase in hybrid poplar. *Plant Biotechnology Journal, 8*, 294-307.

Mansfield, S. D., Mooney, C., & Saddler, J. N. (1999). Substrate and enzyme characteristics that limit cellulose hydrolysis. *Biotechnology Progress, 15*(5), 804-816.

Marin-Rodriguez, M. C., Orchard, J., & Seymour, G. B. (2002). Pectate lyases, cell wall degradation and fruit softening. *Journal of Experimental Botany, 53*(377), 2115-2119.

McQueen-Mason, S. (1995). Expansins and cell wall expansion. *Journal of Experimental Botany, 46*(11), 1639-1650.

Molhoj, M., Ulvskov, P., & Borkhardt, B. (2001). Two arabidopsis thaliana genes, KOR2 and KOR3, which encode membrane-anchored endo-1,4-β-D-glucanases, are differentially expressed in developing leaf trichomes and their support cells. *Plant Molecular Biology, 46*, 263-275.

Murashige, T., & Skoog, F. (1962). A revised medium for rapid growth and bio assays with tobacco tissue cultures. *Physiologia Plantarum, 15*(3), 473-497.

Nicol, F., His, I., Jauneau, A., Vernhettes, S., Canut, H., & Hofte, H. (1998). A plasma membrane-bound putative endo-1,4-[beta]-D-glucanase is required for normal wall assembly and cell elongation in arabidopsis. *The EMBO Journal, 17*(19), 5563-5576.

Nilsson, R., Bernfur, K., Gustavsson, N., Bygdell, J., Wingsle, G., & Larsson, C. (2010). Proteomics of plasma membranes from poplar trees reveals tissue distribution of transporters, receptors, and proteins in cell wall formation. *Molecular & Cellular Proteomics, 9*(2), 368-387.

Peng, L., Kawagoe, Y., Hogan, P., & Delmer, D. (2002). Sitosterol-B-glucoside as primer for cellulose synthesis in plants. *Science, 295*(5552), 147-150.

Persson, S., Caffall, K. H., Freshour, G., Hilley, M. T., Bauer, S., Poindexter, P., et al. (2007). The arabidopsis irregular xylem8 mutant is deficient in glucuronoxylan and homogalacturonan, which are essential for secondary cell wall integrity. *The Plant Cell Online, 19*(1), 237-255.

Persson, S., Paredez, A., Carroll, A., Palsdottir, H., Doblin, M., Poindexter, P., et al. (2007). Genetic evidence for three unique components in primary cell-wall cellulose synthase complexes in arabidopsis. *Proceedings of the National Academy of Sciences, 104*(39), 15566-15571.

Pilate, G., Chabbert, B., Cathala, B., Yoshinaga, A., Leplé, J., Laurans, F., et al. (2004). Lignification and tension wood. *Comptes Rendus Biologies, 327*(9-10), 889-901.

Preston, R. D. (1974). *The physical biology of plant cell walls*. London: Chapman and Hall.

Rose, J. K. C., Braam, J., Fry, S. C., & Nishitani, K. (2002). The XTH family of enzymes involved in xyloglucan endotransglucosylation and endohydrolysis: Current perspectives and a new unifying nomenclature. *Plant and Cell Physiology, 43*(12), 1421-1435.

Schwacke, R., Schneider, A., van, d. G., Fischer, K., Catoni, E., Desimone, M., et al. (2003). ARAMEMNON, a novel database for arabidopsis integral membrane proteins. *Plant Physiology, 131*(1), 16-26.

Shani, Z., Dekel, M., Roiz, L., Horowitz, M., Kolosovski, N., Lapidot, S., et al. (2006). Expression of endo-1,4-β-glucanase (cel1) in arabidopsis thaliana is associated with plant growth, xylem development and cell wall thickening. *Plant Cell Reports, 25*, 1067-1074.

Shoseyov, O., Shani, Z., & Levy, I. (2006). Carbohydrate binding modules: Biochemical properties and novel applications. *Microbiology and Molecular Biology Reviews, 70*(2), 283-295.

Somerville, C. (2006). Cellulose synthesis in higher plants. *Annual Review of Cell and Developmental Biology, 22*(1), 53-78.

Song, D., Xi, W., Shen, J., Bi, T., & Li, L. (2011). Characterization of the plasma membrane proteins and receptor-like kinases associated with secondary vascular differentiation in poplar. *Plant Molecular Biology, 76*(1-2), 97-115.

Szyjanowicz, P. M. J., McKinnon, I., Taylor, N. G., Gardiner, J., Jarvis, M. C., & Turner, S. R. (2004). The irregular xylem 2 mutant is an allele of korrigan that affects the secondary cell wall of arabidopsis thaliana. *The Plant Journal, 37*(5), 730-740.

Taiz, L., & Zeiger, E. (2006). *Plant physiology fourth edition*. Sunderland, MA: Sinauer Associates, Inc.

Taylor, N. G., Gardiner, J. C., Whiteman, R., & Turner, S. R. (2004). Cellulose synthesis in the arabidopsis secondary cell wall. *Cellulose, 11*(3), 329-338; 338.

Taylor, N. G., Howells, R. M., Huttly, A. K., Vickers, K., & Turner, S. R. (2003). Interactions among three distinct CesA proteins essential for cellulose synthesis. *Proceedings of the National Academy of Sciences, 100*(3), 1450-1455.

Teeri, T. T., & Brumer, H. (2003). Discovery, characterisation and applications of enzymes from the wood-forming tissues of poplar: Glycosyl transferases and xyloglucan endotransglycosylases. *Biocatalysis Biotransformation, 21*(4-5), 173-179.

Toufighi, K., Brady, S. M., Austin, R., Ly, E., & Provart, N. J. (2005). The botany array resource: E-northerns, expression angling, and promoter analyses. *The Plant Journal, 43*(1), 153-163.

Trainotti, L., Spolaore, S., Pavanello, A., Baldan, B., & Casadoro, G. (1999). A novel E-type endo-Î²-1,4-glucanase with a putative cellulose-binding domain is highly expressed in ripening strawberry fruits. *Plant Molecular Biology, 40*(2), 323-332; 332.

Turner, S. R., & Somerville, C. R. (1997). Collapsed xylem phenotype of arabidopsis identifies mutants deficient in cellulose deposition in the secondary cell wall. *The Plant Cell Online, 9*(5), 689-701.

Ukrainetz, N. K., Ritland, K., & Mansfield, S. D. (2008). Identification of quantitative trait loci for wood quality and growth across eight full-sib coastal douglas-fir families. *Tree Genetics & Genomes, 4*(2), 159-170.

Updegraff, D. M. (1969). Semimicro determination of cellulose inbiological materials. *Analytical Biochemistry, 32*(3), 420-424.

Urbanowicz, B. R., Catalá, C., Irwin, D., Wilson, D. B., Ripoll, D. R., & Rose, J. K. C. (2007). A tomato endo-β-1,4-glucanase, SlCel9C1, represents a distinct subclass with a new family of carbohydrate binding modules (CBM49). *Journal of Biological Chemistry, 282*(16), 12066-12074.

Verma, D. P. S. (2001). CYTOKINESIS AND BUILDING OF THE CELL PLATE IN PLANTS. *Annual Review of Plant Physiology and Plant Molecular Biology, 52*(1), 751-784.

Vissenberg, K., Fry, S. C., Pauly, M., Hofte, H., & Verbelen, J. (2005). XTH acts at the microfibril-matrix interface during cell elongation. *Journal of Experimental Botany, 56*(412), 673-683.

Vonk, C. G. (1973). Computerization of ruland's X-ray method for determination of the crystallinity in polymers. *Journal of Applied Crystallography, 6*(2), 148-152.

Wasteneys, G., & Fujita, M. (2006). Establishing and maintaining axial growth: Wall mechanical properties and the cytoskeleton. *Journal of Plant Research, 119*(1), 5-10.

Whitney, S. E. C., Gothard, M. G. E., Mitchell, J. T., & Gidley, M. J. (1999). Roles of cellulose and xyloglucan in determining the mechanical properties of primary plant cell walls. *Plant Physiology, 121*(2), 657-664.

Wilson, D. B., & Urbanowicz, B. (2010). *Glycoside hydrolase family 9.* Retrieved August 24, 2010, from http://www.cazypedia.org/

Winter, D., Vinegar, B., Nahal, H., Ammar, R., Wilson, G. V., & Provart, N. J. (2007). An electronic fluorescent pictograph browser for exploring and analyzing large-scale biological data sets. *PLoS ONE, 2*(8), e718.

Xie, X., Huang, J., Gao, H., & Guo, G. (2011). Expression patterns of two arabidopsis endo-beta-1,4-glucanase genes (At3g43860, At4g39000) in reproductive development. *Molecular Biology, 45*(3), 458-465.

Yoshida, K., Imaizumi, N., Kaneko, S., Kawagoe, Y., Tagiri, A., Tanaka, H., et al. (2006a). Carbohydrate-binding module of a rice endo-β-1,4-glycanase, OsCel9A, expressed in auxin-induced lateral root primordia, is post-translationally truncated. *Plant & Cell Physiology, 47*(11), 1555-1571.

Yoshida, K., & Komae, K. (2006b). A rice family 9 glycoside hydrolase isozyme with broad substrate specificity for hemicelluloses in type II cell walls. *Plant and Cell Physiology, 47*(11), 1541-1554.

Zhong, R., Lee, C., Zhou, J., McCarthy, R. L., & Ye, Z. (2008). A battery of transcription factors involved in the regulation of secondary cell wall biosynthesis in arabidopsis. *The Plant Cell Online, 20*(10), 2763-2782.